NACA

RESEARCH MEMORANDUM

FULL-SCALE WIND-TUNNEL TESTS OF A 35° SWEPTBACK-WING AIRPLANE WITH HIGH-VELOCITY BLOWING OVER THE TRAILING-EDGE FLAPS - LONGITUDINAL AND LATERAL STABILITY AND CONTROL

By William H. Tolhurst, Jr., and Mark W. Kelly

Ames Aeronautical Laboratory
Moffett Field, Calif.

NATIONAL ADVISORY COMMITTEE
FOR AERONAUTICS

WASHINGTON

October 5, 1956

NATIONAL ADVISORY COMMITTEE FOR AERONAUTICS

RESEARCH MEMORANDUM

FULL-SCALE WIND-TUNNEL TESTS OF A 35° SWEPTBACK-WING AIRPLANE WITH HIGH-VELOCITY BLOWING OVER THE TRAILING-EDGE FLAPS - LONGITUDINAL AND LATERAL STABILITY AND CONTROL

By William H. Tolhurst, Jr., and Mark W. Kelly

SUMMARY

A wind-tunnel investigation was made to determine the effects of a blowing type boundary-layer control flap on the longitudinal control and lateral stability and control of an F-86D airplane. The results are presented as six-component force data measured at a Reynolds number of 7.5×10^6.

The results showed that blowing over the deflected flap increased the average downwash angle at the horizontal tail. With this increase in downwash angle, however, the horizontal tail was not near stall at trim conditions of interest during take-off or landing. The lateral stability exhibited an increase in effective dihedral and in directional stability with blowing over the flap. With the flaps deflected to 60°, blowing over the flaps also increased the aileron effectiveness approximately 25 percent at the maximum aileron deflection angles.

Tests were made also of the following types of lateral control devices: split-flap-type spoilers, differentially deflected flaps, and differential amounts of blowing over the flaps.

INTRODUCTION

The investigation reported in reference 1 showed the lift, drag, and pitching-moment changes resulting from the use of blowing boundary-layer control flaps on the YF-86D airplane. Reported herein are the results of additional tests to examine the effects of the blowing flaps on the longitudinal control and lateral stability and control of the same airplane. Also reported are the results of tests to determine the effectiveness of the following types of lateral control devices: split-flap-type spoilers, differentially deflected flaps, and differential amounts of blowing over the flaps.

Wind-tunnel data have been presented in references 2 and 3 which show that the wing leading-edge slats which are standard equipment on the F-86 airplane may be replaced, without loss in maximum lift, by a fixed leading edge having an increased nose radius and leading-edge camber. The modified leading edge was tested in flight (refs. 4 and 5) and was found to have objectionable roll-off characteristics at the stall. It was found during the flight tests that the installation of a fence on the leading edge at the 0.628 semispan station alleviated the undesirable roll-off characteristics.

In the above investigations, stability and control characteristics were determined for the leading-edge modification in conjunction with a single-slotted flap (refs. 2 and 4) and with the area-suction-type boundary-layer-control flap (refs. 3 and 5). In the present investigation, this same modification was tested with and without the fence to determine the stability characteristics in conjunction with the blowing-type boundary-layer-control flap. Except for the tests evaluating the modified leading edge and fence, the standard F-86 leading edge with the slats locked in the retracted position was used throughout the investigation.

NOTATION

A area, sq ft

b wing span, ft

c wing chord, parallel to plane of symmetry, ft

$\bar{c}$ mean aerodynamic chord, $\frac{2}{S}\int_0^{b/2} c^2 dy$, ft

c_t horizontal-tail chord, parallel to plane of symmetry, ft

C_D drag coefficient, $\frac{\text{drag}}{q_\infty S}$

C_L lift coefficient, $\frac{\text{lift}}{q_\infty S}$

C_m pitching-moment coefficient, $\frac{\text{pitching moment}}{q_\infty S\bar{c}}$

C_l rolling-moment coefficient, $\frac{\text{rolling moment}}{q_\infty Sb}$

C_n yawing-moment coefficient, $\frac{\text{yawing moment}}{q_\infty Sb}$

C_Y side-force coefficient, $\frac{\text{side force}}{q_\infty S}$

C_μ momentum coefficient, $\frac{W_j/g}{q_\infty S} V_j$

ΔC_μ difference of right and left flap momentum coefficient

d distance from engine thrust line to moment center, ft

F_G gross thrust from engine, $\frac{W_E V_{TP}}{g}$, lb

F_N net thrust from engine, $F_G - \frac{W_E U_\infty}{g}$, lb

g acceleration of gravity, 32.2 ft/sec^2

i_t horizontal-tail incidence angle, deg

L.E. leading edge

p static pressure, lb/sq ft

p_d total pressure in flap duct, lb/sq ft

p_t total pressure, lb/sq ft

q dynamic pressure, lb/sq ft

R gas constant for air, 1715 sq ft/sec^2, deg Rankine

S wing area, sq ft

T temperature, deg Rankine

U velocity, ft/sec

V_{TP} velocity at tail-pipe exit, ft/sec

V_j jet velocity assuming isentropic expansion,

$$\sqrt{\frac{2\gamma}{\gamma - 1} RT_d \left[1 - \left(\frac{p_\infty}{p_d}\right)^{\frac{\gamma-1}{\gamma}}\right]}, \text{ ft/sec}$$

W weight rate of flow, lb/sec

y	lateral distance from vertical plane of symmetry, ft
α	angle of attack of fuselage reference line, deg
β	sideslip angle, deg
γ	ratio of specific heats, 1.4 for air
δ_a	aileron deflection, measured in plane normal to aileron hinge line, deg
δ_f	flap deflection, measured in plane normal to flap hinge line, deg
$\Delta\delta_f$	difference of right and left flap deflection, deg
δ_s	spoiler deflection, measured normal to spoiler hinge line, deg
ϵ	angle between engine tail pipe and fuselage reference line, deg ($+6.5^\circ$)
φ	angle between flap nozzle and a line through the flap hinge line perpendicular to the flap chord plane (see fig. 3(b))

Subscripts

∞	free stream
d	trailing-edge-flap ducts
E	engine
f	trailing-edge flaps
i	engine inlet
j	flap jet
L	left
R	right
u	uncorrected

MODEL AND APPARATUS

The model consisted of a YF-86D airplane on which the standard single-slotted flaps were replaced by plain flaps with blowing boundary-layer control. A photograph of the model mounted in the Ames 40- by 80-foot wind tunnel is shown in figure 1. A sketch showing the major dimensions and geometric parameters of importance is presented in figure 2. The airfoil section at the wing root was an NACA 0012-64 (modified) and at the wing tip was an NACA 0011-64 (modified). Table I contains the airfoil section ordinates at two spanwise stations. The horizontal tail, also shown in figure 2, was all-movable with the elevator locked in the undeflected position.

Details of the wing with the various lateral control devices and the blowing flap are shown in figure 3. A section view of the modified leading edge and details of the fence are shown in figure 4. Coordinates of the modified wing leading edge at two span stations are given in table II. The fence was installed on the modified leading edge parallel to the windstream at the 0.628 semispan station.

TESTS

Method of Testing

The tests were conducted at a Reynolds number of 7.5×10^6 which corresponds to a dynamic pressure of 25 pounds per square foot. The angle of attack was varied from -2° to $+20^\circ$ and the angle of sideslip from 0° to $+8^\circ$. The flap blowing momentum coefficients were varied from 0 to 0.018.

The effect of the blowing flap on the longitudinal control was determined by varying the airplane angle of attack with the horizontal tail set at various angles of incidence from $+3^\circ$ to -9.8°. The dynamic pressure at the horizontal tail was measured by shielded total-head tubes located near the leading edge of the tail. After completion of the longitudinal control tests, the horizontal tail was removed from the airplane and all other tests were conducted with the tail off but the vertical tail remained on throughout the entire test program. Unless otherwise stated all tests were made with the slatted leading edge retracted and sealed.

The effects of the blowing flaps on the lateral stability characteristics were investigated by varying the angle of attack at constant angles of sideslip with the flaps undeflected and deflected 60°.

The effectiveness of the various lateral control devices was determined by varying the angle of attack and operating the control on the right wing only. The aileron deflection angle was varied from -15° to $+15^\circ$. The

spoiler was varied from 0° to 60° deflection angle with the spanwise extent varying from 0.47 semispan to 0.87 semispan measured from the wing tip. For the differentially deflected flaps the left flap was deflected a constant 45° with the right flap varying from 25° to 75°, and with the left flap at a constant 60° the right flap was varied from 25° to 85°. For the differential blowing tests, both flaps were deflected to 60° and the jet momentum coefficient was varied on the right flap from C_μ = 0 to 0.012 while the momentum coefficient on the left flap was held constant at C_μ = 0.006. The flap nozzle was located at an angular setting (φ) of 22.5° when the flaps were deflected to 45° and at 30° when the flaps were deflected to 60°, except during the tests with the flaps deflected differentially. In these tests, the angle φ was held constant on the right flap as it was deflected through the angle range.

Measurement of Engine Thrust

Since the source of high-pressure air for the flap nozzles was a turbojet engine mounted in the fuselage, it was necessary to correct the measured force data for the effects of engine thrust. The gross thrust was obtained from a static-thrust calibration using the tunnel balance system. The net thrust was obtained by subtracting the ram drag from the gross thrust.

$$F_N = F_G - \frac{W_E U_\infty}{g}$$

The weight rate of flow through the engine, W_E, was obtained from pressure measurements at the engine compressor inlet by the following equation:

$$W_E = A_i \sqrt{\frac{2\gamma}{\gamma - 1} \frac{(gp_i)^2}{RT_i} \left[\left(\frac{p_t}{p} \right)_i^{\frac{\gamma-1}{\gamma}} - 1 \right]}$$

A more detailed discussion of these measurements will be found in reference 1.

CORRECTIONS

The force data obtained from the wind-tunnel balance system were not corrected for support-strut interference but were corrected for the effects of the wind-tunnel-wall interference as follows:

$$\alpha = \alpha_u + 0.611\ C_{L_u}$$

$$C_D = C_{D_u} + 0.0107\ C_{L_u}^2$$

$$C_m = C_{m_u} + 0.00691\ C_{L_u} \text{ (for tail-on tests only)}$$

The following corrections for the effects of the engine thrust were made:

$$C_L = \frac{\text{total lift}}{q_\infty S} - \frac{F_N}{q_\infty S} \sin(\alpha + \epsilon)$$

$$C_D = \frac{\text{total drag}}{q_\infty S} + \frac{F_N}{q_\infty S} \cos(\alpha + \epsilon)$$

$$C_m = \frac{\text{total moment}}{q_\infty S \bar{c}} + \frac{F_N d}{q_\infty S \bar{c}}$$

$$C_Y = \frac{\text{total side force}}{q_\infty S} + \frac{F_N}{q_\infty S} \cos(\alpha + \epsilon) \sin \beta$$

$$C_l = \frac{\text{total rolling moment}}{q_\infty S b} - \frac{\bar{c}}{b} \frac{F_N d}{q_\infty S \bar{c}} \sin \beta + \left(\frac{F_N d}{q_\infty S b} \sin \beta \right) \cos \beta$$

RESULTS AND DISCUSSION

Longitudinal Control

The investigation previously reported in reference 1 was primarily concerned with the development of the plain flap with blowing boundary-layer control on the YF-86D airplane. The data presented in that report showed the effects of the blowing flap on the longitudinal stability of the airplane. The investigation was continued, as reported herein, with the horizontal tail set at various angles of incidence and the effects of the blowing flaps on the longitudinal control characteristics were determined.

Figure 5(a) shows the longitudinal characteristics of the airplane with the flaps deflected 45° with no boundary-layer control. Figure 5(b) shows the characteristics with blowing over the flaps at a constant momentum coefficient. (The momentum coefficient was held constant at a value which would insure boundary-layer control on the flap throughout the angle-of-attack range.) Figures 6(a) and 6(b) show similar data for the flaps

deflected to 60°. Tail-off data are presented in addition to the tail-on data in order to evaluate the average downwash angle at the horizontal tail. The change in the average downwash angle at the tail was computed from these data. It was found that blowing over the flaps increased the downwash angle approximately 3.5° with the flaps deflected to 45° and approximately 4.5° with the flaps at 60°. (The measured total-head ratio at the tail remained unity for all angles of attack and flap deflections when boundary-layer control was applied to the flap.) Although the downwash angle at the tail was increased by the blowing flap, the data indicate that the horizontal tail was not near the stall for trim conditions in the flight range of interest during take-off and landing.

Lateral Stability

The effects of deflecting the flaps to 60° and of blowing over the flap on the aerodynamic characteristics of the airplane at various angles of sideslip is shown in figure 7. These results indicate that there is a small increase in both dihedral effect and directional stability. (As mentioned previously in "Tests" all lateral stability and control data were measured with the horizontal tail off.)

Lateral Control

Ailerons.- The effect of aileron deflection on the aerodynamic characteristics of the airplane with undeflected flaps is shown in figure 8. Figure 9 shows the effect of aileron deflection when the flaps are deflected to 60° both with and without blowing over the flaps. A comparison in figure 10 shows that with the flap deflected 60° blowing over the flap increases the aileron effectiveness by an almost constant increment which amounts to approximately 25 percent at the maximum deflection angle. An increase in aileron effectiveness by flap blowing has also been noted in unpublished pilot comments pertaining to flights of an airplane of this type equipped with blowing boundary-layer-control flaps.

Spoilers.- The effectiveness of spoilers as a lateral control device is shown in figures 11 through 20. The data presented in figures 11 through 16 were obtained with no blowing over the trailing-edge flaps and show characteristics typical of spoiler controls. The data presented in figures 17 through 20 were obtained with blowing over the flaps and it may be seen that with the full-span spoiler large nonlinearities in the curves of rolling moment as a function of spoiler deflection were obtained. These nonlinearities resulted when the spoiler ahead of the flap was deflected a sufficient amount to overcome the flap boundary-layer control and thus stall the flap.

The amount of nonlinearity could, of course, be reduced by reducing the amount of spoiler operating ahead of the flap. Reducing the span of the spoiler to 0.55 semispan (fig. 19(b)) decreased the amount of nonlinearity and still retained rolling moments which were comparable to those of the standard aileron (fig. 8(b)). Reduction of the spoiler span to 0.47 semispan (fig. 20(b)) further reduced the nonlinearity but resulted in rolling moments which were less than those of the aileron.

Differential flap deflection.- The effectiveness of differentially deflected flaps as a roll control device is shown in figures 21 through 25. The data of figures 21 and 23 were obtained with no boundary-layer control on the flaps while the data of figures 22 and 24 were obtained by maintaining C_μ equal and constant on each flap. In these latter figures it is seen that as the right-hand flap was deflected from the minimum angle ($\delta_f = 25^\circ$) downward there was an angle at which the C_μ was not sufficient to retain boundary-layer control and there was a reversal in roll direction. When these data are compared with the data of reference 1 (fig. 16(a)) it is seen that the right flap stalls at a lower deflection angle than would be expected from the data of reference 1. In the present test the angle φ was held constant at the position dictated by the minimum pressure location (ref. 1, p. 14) when the flaps were set at equal deflection angles. When the deflection angle of the right flap was increased, the nozzle moved behind the minimum pressure peak and the momentum of the jet was insufficient to control separation. As shown in figure 25, when the value of C_μ was increased with increasing flap deflection angle to maintain boundary-layer control throughout the angle range, the reversal in roll direction was eliminated and rolling moments comparable to those of the standard aileron (fig. 8(b)) were developed.

Differential flap blowing.- The effects of blowing differentially over the flaps is shown in figure 26. The effectiveness of this method of control depended on the manner in which it was applied. When the C_μ on one flap was increased above the amount required for boundary-layer control, insignificant rolling moments were developed within the available C_μ range. When the C_μ was reduced and separation occurred on the flap significant rolling moments were developed.

Wing Leading-Edge Modification

As discussed in the introduction, wind-tunnel and flight investigations have been made (refs. 2 to 5) which show that the standard F-86 wing leading-edge slats may be replaced by a fixed leading edge having an increased nose radius and camber. The modified leading edge was found to increase the maximum lift obtainable but at the stall there was an objectionable roll-off which was subsequently relieved by the installation of a fence at the 0.628 semispan station. This leading edge, having been tested with both a single-slotted flap and an area-suction-type

boundary-layer-control flap, was tested during the present investigation to evaluate it, with and without the fence, with the blowing-type flap.

The aerodynamic characteristics of the airplane with the modified leading edge are compared, in figure 27, with data from reference 1 showing the characteristics of the airplane with the standard slats extended. The effects of adding the fences to the modified leading edges are shown for the flaps deflected 60° without and with blowing on the flaps. As in the previous tests (refs. 2 and 3), $C_{L_{max}}$ was increased by the leading edge modification but the stall was accompanied by a severe roll-off and an unstable pitching-moment break. Addition of the fences resulted in almost complete elimination of the roll-off, but the maximum lift was reduced to a value that nullified the gains made by the modified leading edge.

CONCLUDING REMARKS

The investigation of the effects of blowing-flap boundary-layer control on the longitudinal control of the YF-86D airplane indicated that the average downwash angle at the horizontal tail was increased approximately 3.5° and 4.5° by blowing over the flaps deflected 45° and 60°, respectively. With this increase in downwash angle, however, the lift of the horizontal tail was not near stall at trim conditions of interest during landing or take-off.

The lateral stability was increased slightly by blowing over the flaps. With the flaps deflected 60°, blowing over the flaps increased the effectiveness of the ailerons by approximately 25 percent at the maximum aileron angle.

Tests of alternate lateral control devices indicated that spoilers used in conjunction with blowing-type flaps would give roll control comparable to that of the standard aileron. Roll control by means of differentially deflected flaps was also found to be feasible; however, roll control by differential amounts of blowing on the flaps did not produce rolling moments comparable to those of the aileron until one flap was completely stalled.

The lift increase developed by the use of a modified leading edge was nullified when fences were installed to minimize the sharp stall and roll-off.

Ames Aeronautical Laboratory
National Advisory Committee for Aeronautics
Moffett Field, Calif., May 24, 1956

REFERENCES

1. Kelly, Mark W., and Tolhurst, William H., Jr.: Full-Scale Wind-Tunnel Tests of a 35° Sweptback Wing Airplane With High-Velocity Blowing Over the Trailing-Edge Flaps. NACA RM A55I09, 1955.

2. Maki, Ralph L.: Full-Scale Wind-Tunnel Investigation of the Effects of Wing Modifications and Horizontal-Tail Location on the Low-Speed Static Longitudinal Characteristics of a 35° Swept-Wing Airplane. NACA RM A52B05, 1952.

3. Cook, Woodrow L., Holzhauser, Curt A., and Kelly, Mark W.: The Use of Area Suction for the Purpose of Improving Trailing-Edge Flap Effectiveness on a 35° Sweptback Wing. NACA RM A53E06, 1953.

4. Anderson, Seth B., Matteson, Frederick H., and Van Dyke, Rudolph D., Jr.: A Flight Investigation of the Effects of Leading-Edge Camber on the Aerodynamic Characteristics of a Swept-Wing Airplane. NACA RM A52L16a, 1953.

5. Anderson, Seth B., and Quigley, Hervey C.: Flight Measurements of the Low-Speed Characteristics of a 35° Swept-Wing Airplane With Area-Suction Boundary-Layer Control on the Flaps. NACA RM A55K29, 1956.

TABLE I.- COORDINATES OF THE WING AIRFOIL SECTIONS NORMAL TO THE WING QUARTER-CHORD LINE AT TWO SPAN STATIONS
[Dimensions given in inches]

Section at 0.467 semispan			Section at 0.857 semispan		
Distance from L.E.	Ordinate		Distance from L.E.	Ordinate	
	Upper	Lower		Upper	Lower
0	0.231	---	0	-0.098	---
.119	.738	-0.307	.089	.278	-0.464
.239	.943	-.516	.177	.420	-.605
.398	1.127	-.698	.295	.562	-.739
.597	1.320	-.895	.443	.701	-.879
.996	1.607	-1.196	.738	.908	-1.089
1.992	2.104	-1.703	1.476	1.273	-1.437
3.984	2.715	-2.358	2.952	1.730	-1.878
5.976	3.121	-2.811	4.428	2.046	-2.176
7.968	3.428	-3.161	5.903	2.290	-2.401
11.952	3.863	-3.687	8.855	2.648	-2.722
15.936	4.157	-4.064	11.806	2.911	-2.944
19.920	4.357	-4.364	14.758	3.104	-3.102
23.904	4.480	-4.573	17.710	3.244	-3.200
27.888	4.533	-4.719	20.661	3.333	-3.250
31.872	4.525	-4.800	23.613	3.380	-3.256
35.856	4.444	-4.812	26.564	3.373	-3.213
39.840	4.299	-4.758	29.516	3.322	-3.126
43.825	4.081	-4.638	32.467	3.219	-2.989
47.809	3.808	-4.452	35.419	3.074	-2.803
51.793	3.470	-4.202	38.370	2.885	-2.574
55.777	3.066	-3.891	41.322	2.650	-2.302
59.761	2.603	-3.521	44.273	2.374	-1.986
[a]63.745	2.079	-3.089	[a]47.225	2.054	-1.625
83.681	-.740	---	63.031	.321	---
L.E. radius: 1.202, center at (1.202, 0.216)			L.E. radius: 0.822, center at (0.822, -0.093)		

[a]Straight lines to trailing edge

TABLE II.- COORDINATES OF THE MODIFIED WING LEADING EDGE AT TWO SPAN STATIONS NORMAL TO THE WING QUARTER-CHORD LINE
[Dimensions given in inches]

Section at 0.467 semispan			Section at 0.857 semispan		
Distance from L.E.	Ordinate		Distance from L.E.	Ordinate	
	Upper	Lower		Upper	Lower
-1.692	-1.445	---	-1.250	-1.359	---
-1.273	-.348	-2.552	-.934	-.495	-2.192
-.855	.222	-2.898	-.619	-.099	-2.454
-.436	.629	-3.114	-.304	.197	-2.609
-.018	.969	-3.272	.011	.456	-2.701
.400	1.266	-3.391	.326	.675	-2.769
.819	1.527	-3.473	.641	.867	-2.796
1.237	1.760	-3.523	.956	1.040	-2.813
1.655	1.952	-3.549	1.272	1.189	-2.821
1.992	2.104	- - -	1.476	1.273	---
2.074	---	-3.552	1.587	---	-2.813
2.911	---	-3.531	2.217	---	-2.787
4.166	---	-3.481	3.163	---	-2.742
6.258	---	-3.472	4.739	---	-2.709
8.350	---	-3.542	6.314	---	-2.712
10.442	---	-3.657	7.890	---	-2.751
14.626	---	-3.956	9.466	---	-2.808
15.936	---	-4.064	11.042	---	-2.885
			11.806	---	-2.944
L.E. radius: 1.674, center at (-0.018, -1.445)			L.E. radius: 1.261, center at (0.011, -1.359)		

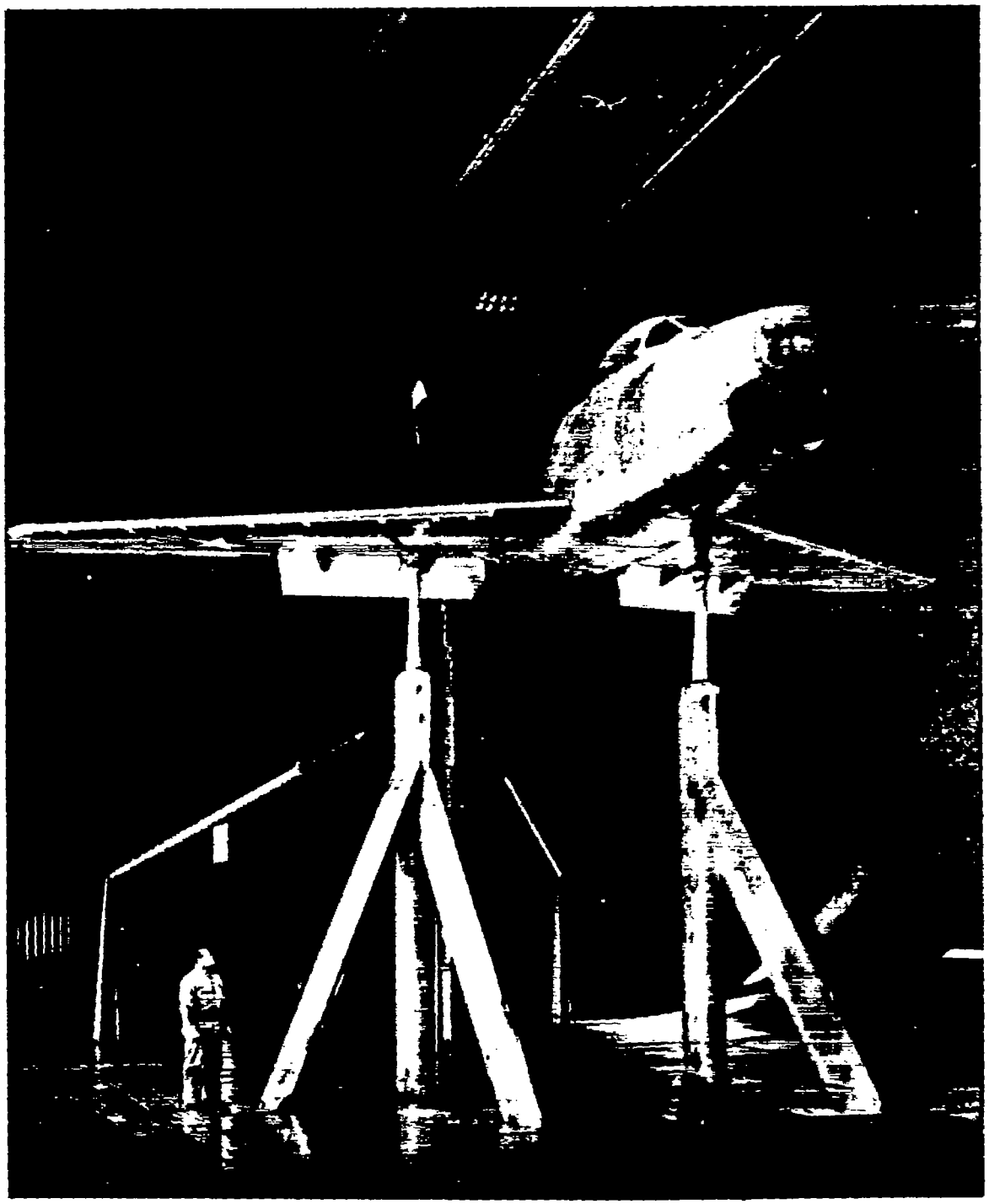

A-19719

Figure 1.- Photograph of YF-86D airplane mounted in the Ames 40- by 80-foot wind tunnel.

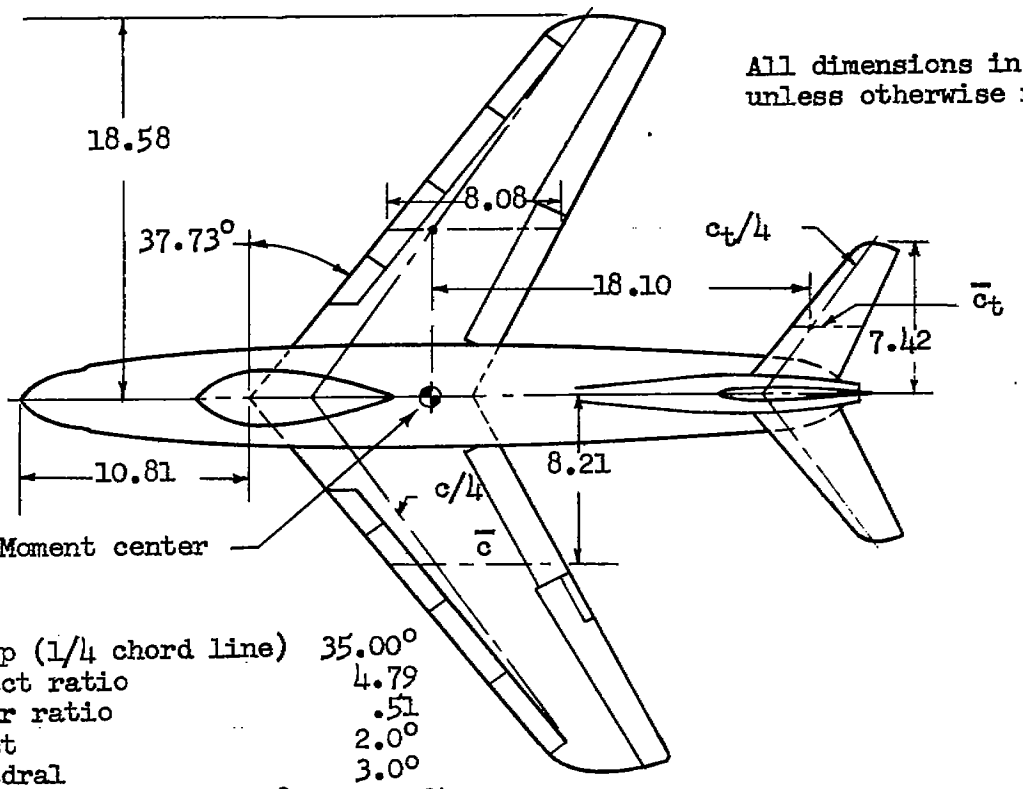

Wing	
Sweep (1/4 chord line)	35.00°
Aspect ratio	4.79
Taper ratio	.51
Twist	2.0°
Dihedral	3.0°
Area	287.90 sq ft

Horizontal Tail	
Sweep	35.00°
Aspect ratio	4.73
Taper ratio	.451
Twist	0°
Dihedral	0°
Area	46.5 sq ft

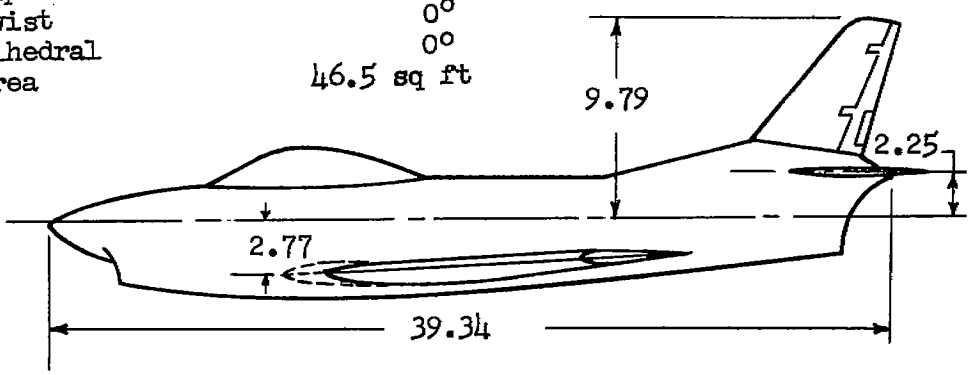

Figure 2.- General arrangement of YF-86D airplane.

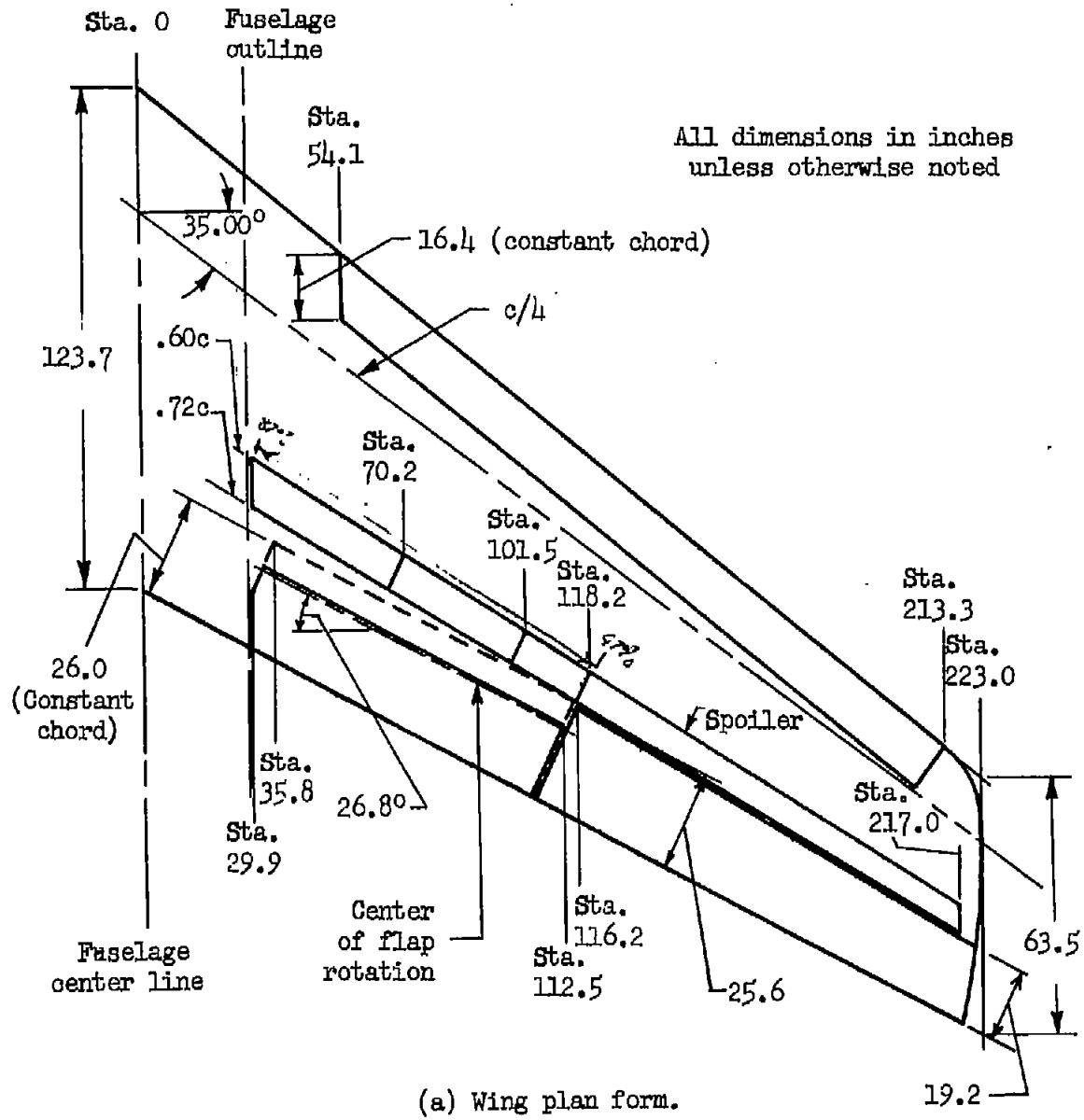

(a) Wing plan form.

Figure 3.- Details of wing with lateral control devices and blowing flap.

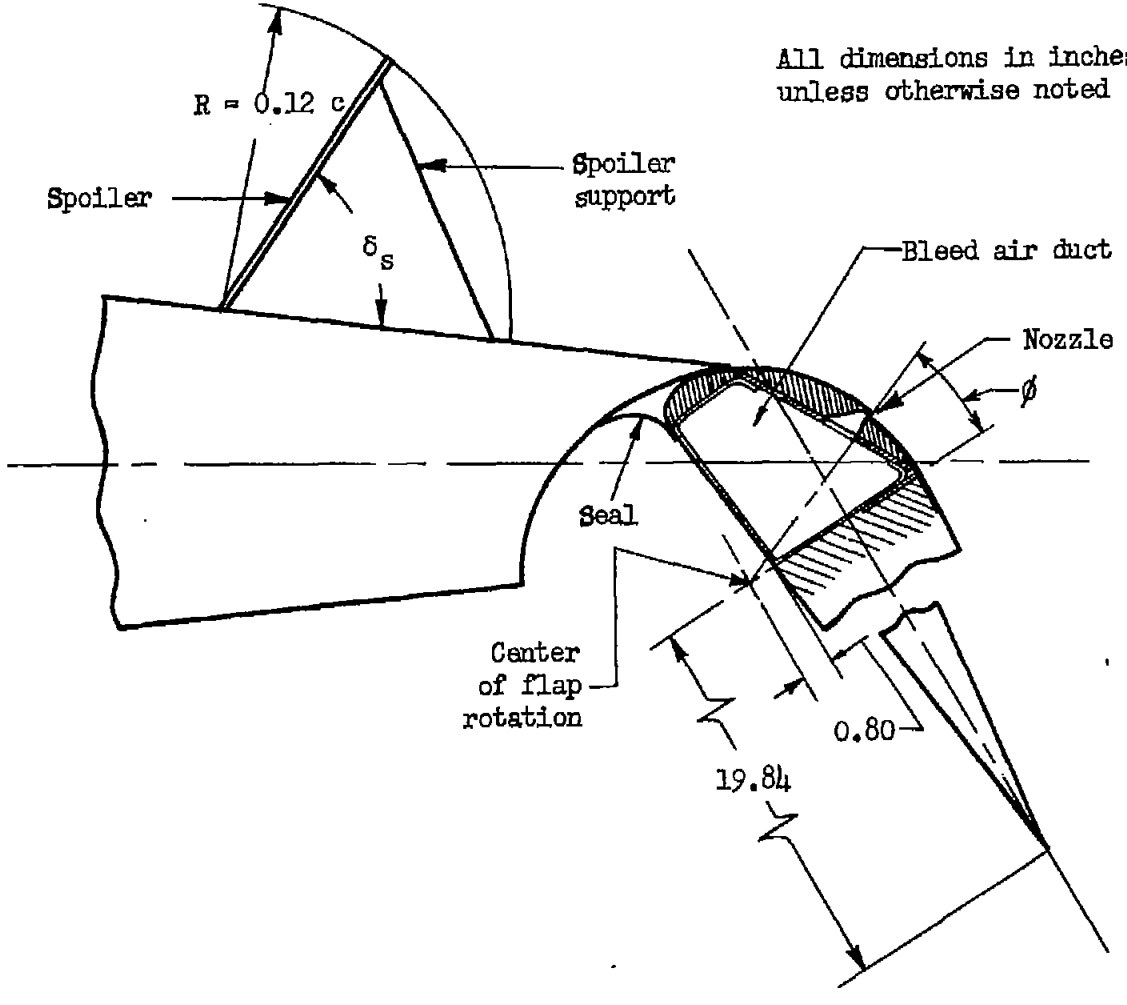

(b) Section view of blowing flap and spoiler.

Figure 3.- Concluded.

Dimensions in feet

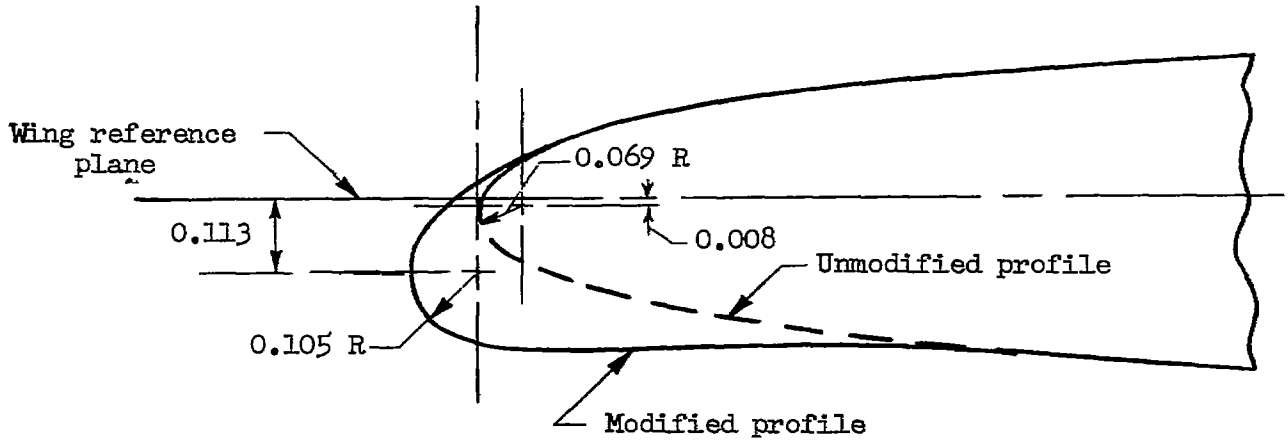

(a) Airfoil section at 0.857 semispan normal to wing quarter-chord line.

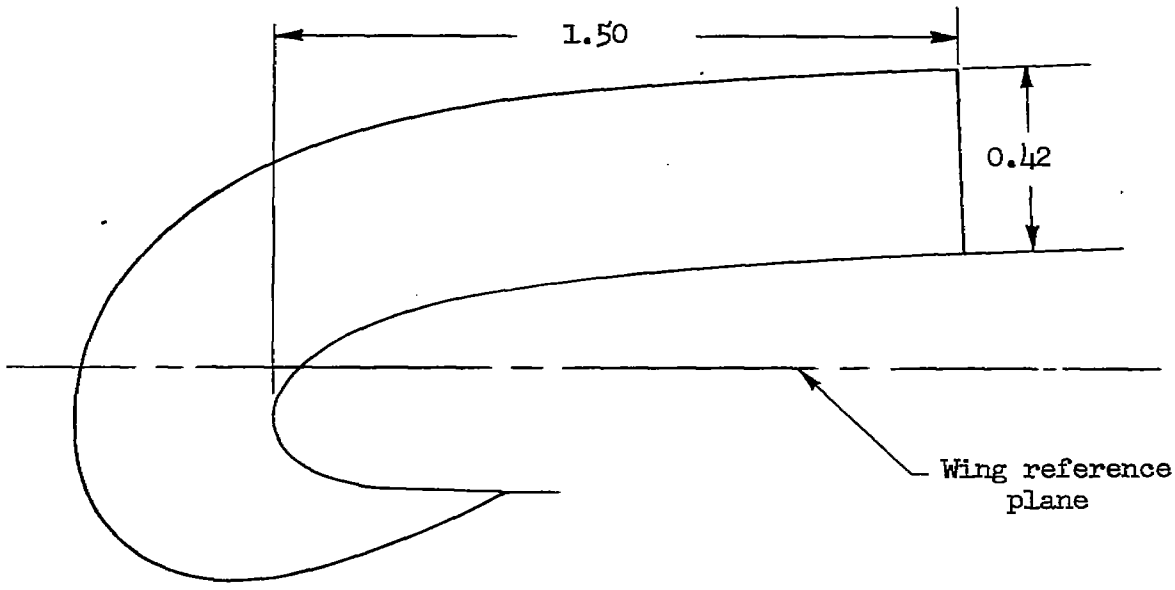

(b) Fence located at 0.628 semispan.

Figure 4.- Details of modified wing leading edge and fence.

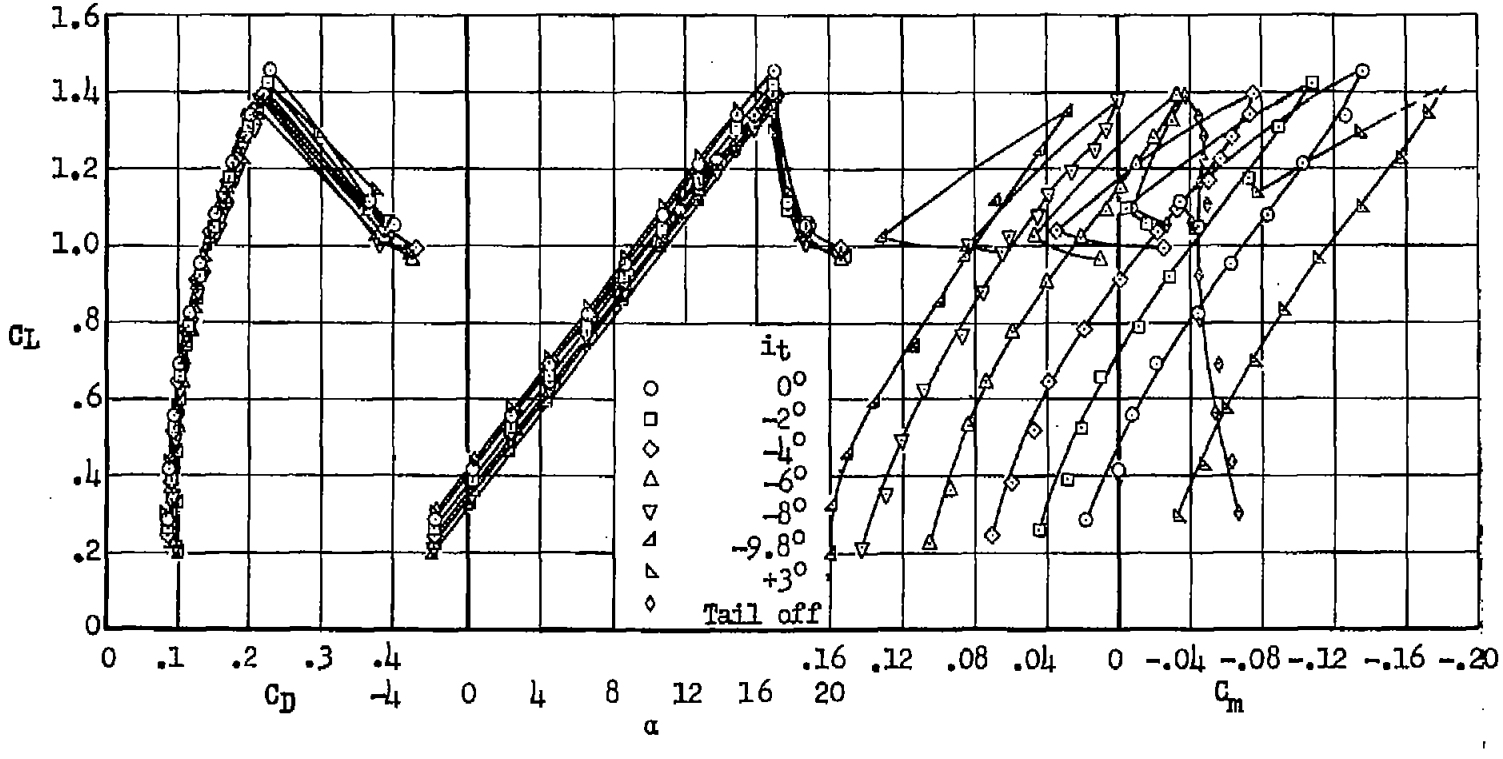

(a) Blowing off.

Figure 5.- Aerodynamic characteristics of the airplane with the horizontal tail; $\delta_f = 45°$.

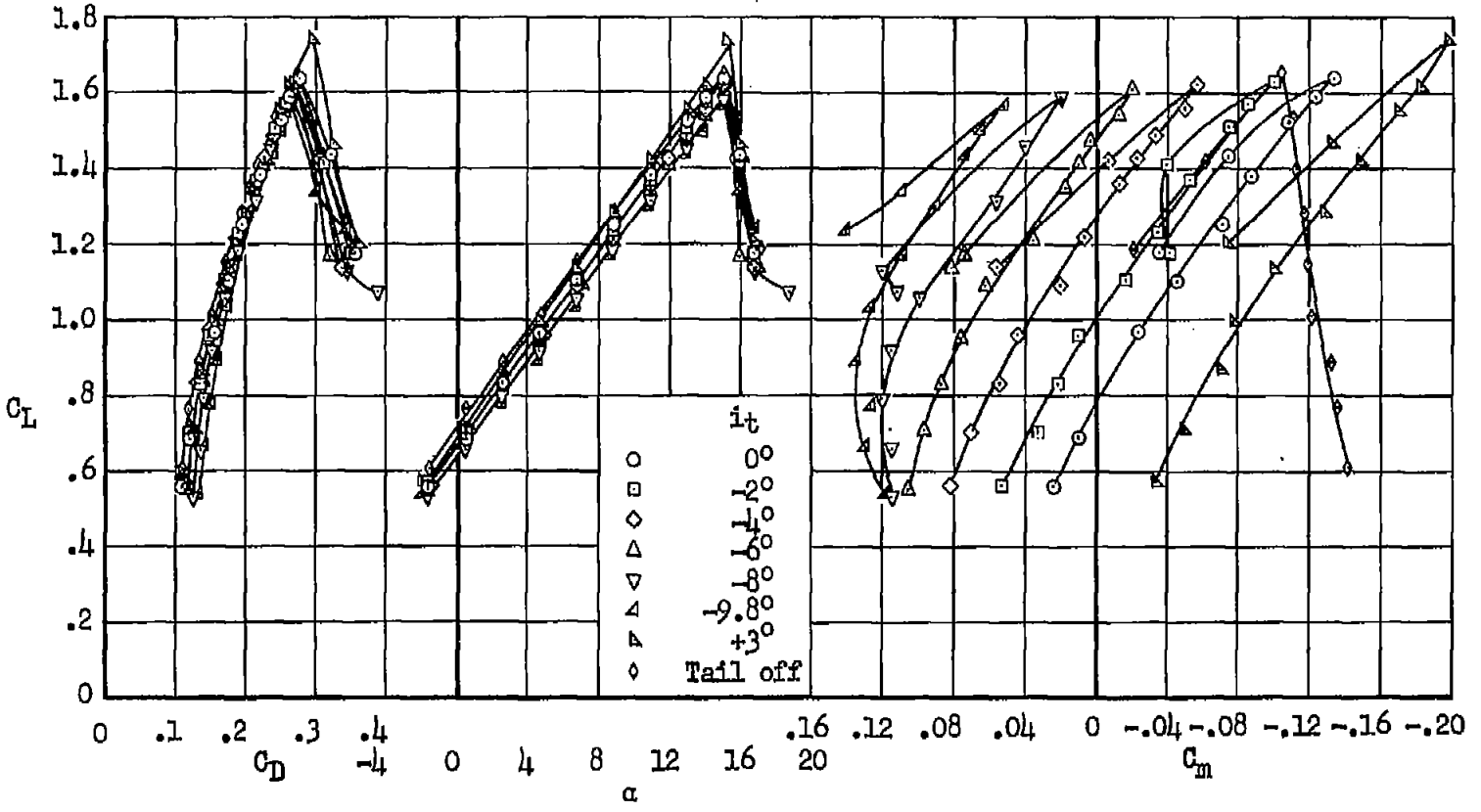

(b) Blowing on; C_μ = 0.012.

Figure 5.- Concluded.

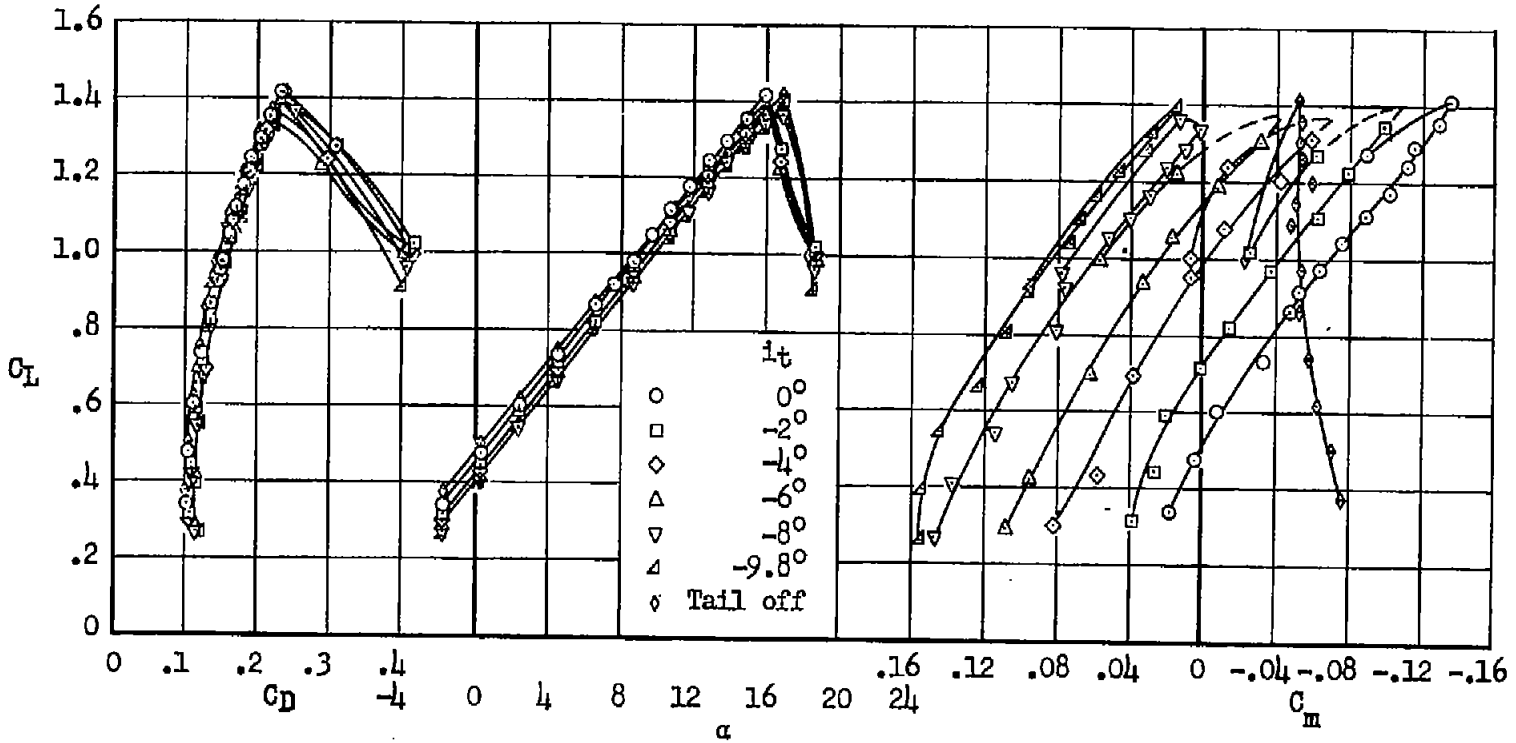

(a) Blowing off.

Figure 6.- Aerodynamic characteristics of the airplane with the horizontal tail; $\delta_f = 60°$.

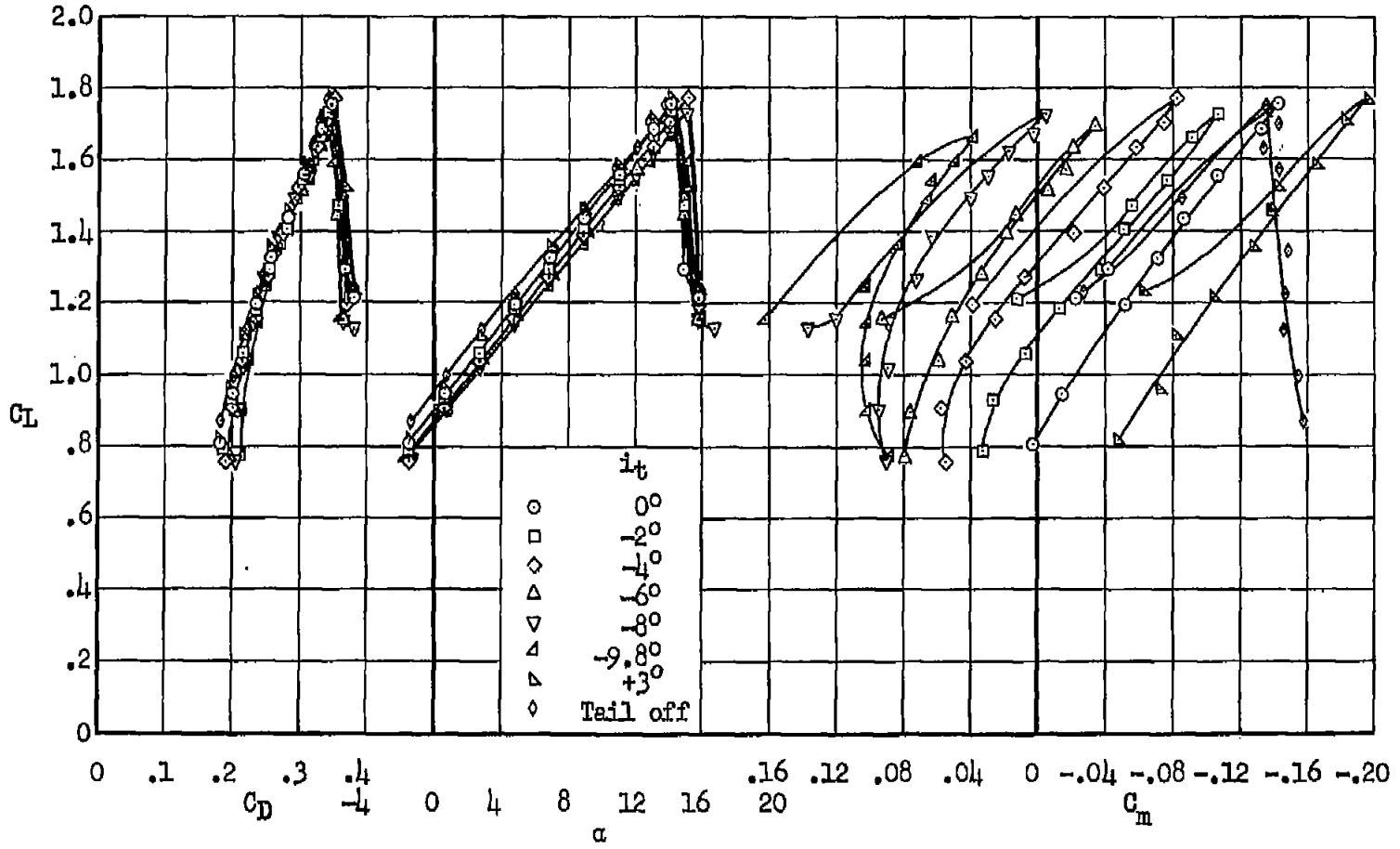

(b) Blowing on; C_μ = 0.017.

Figure 6.- Concluded.

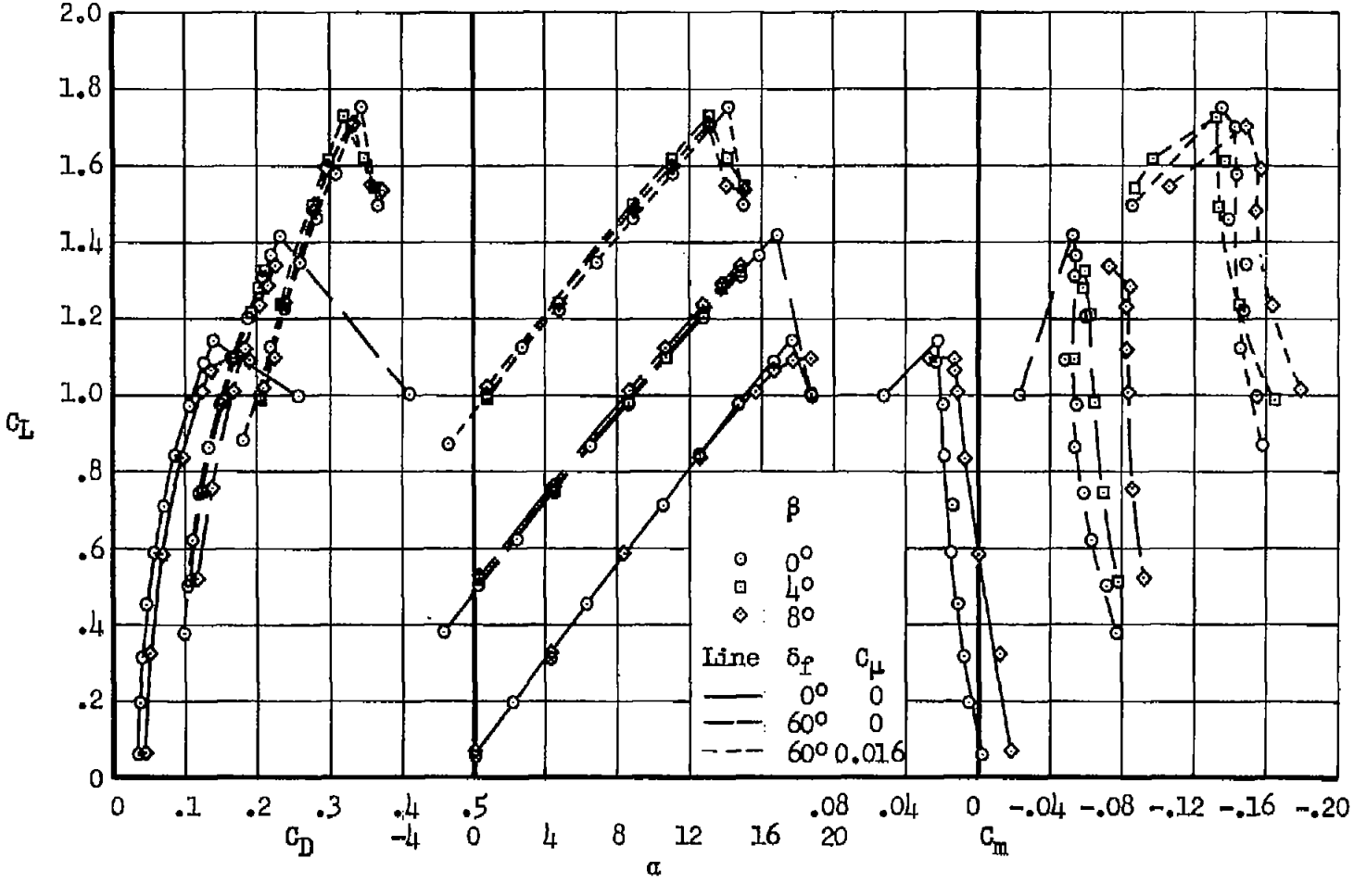

(a) Longitudinal characteristics.

Figure 7.- Effect of flap deflection and flap blowing on the aerodynamic characteristics of the airplane at various sideslip angles.

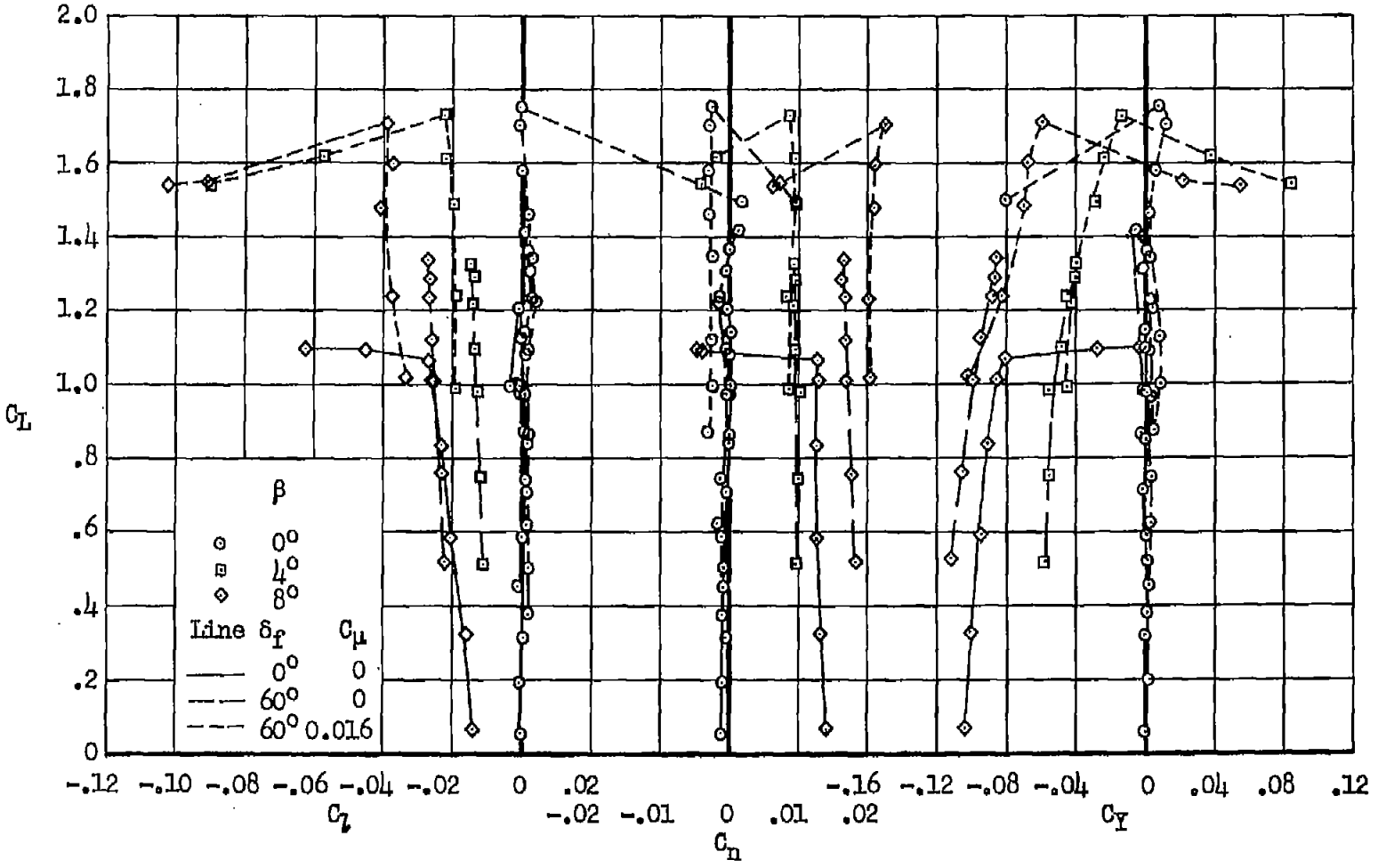

(b) Lateral characteristics.

Figure 7.- Concluded.

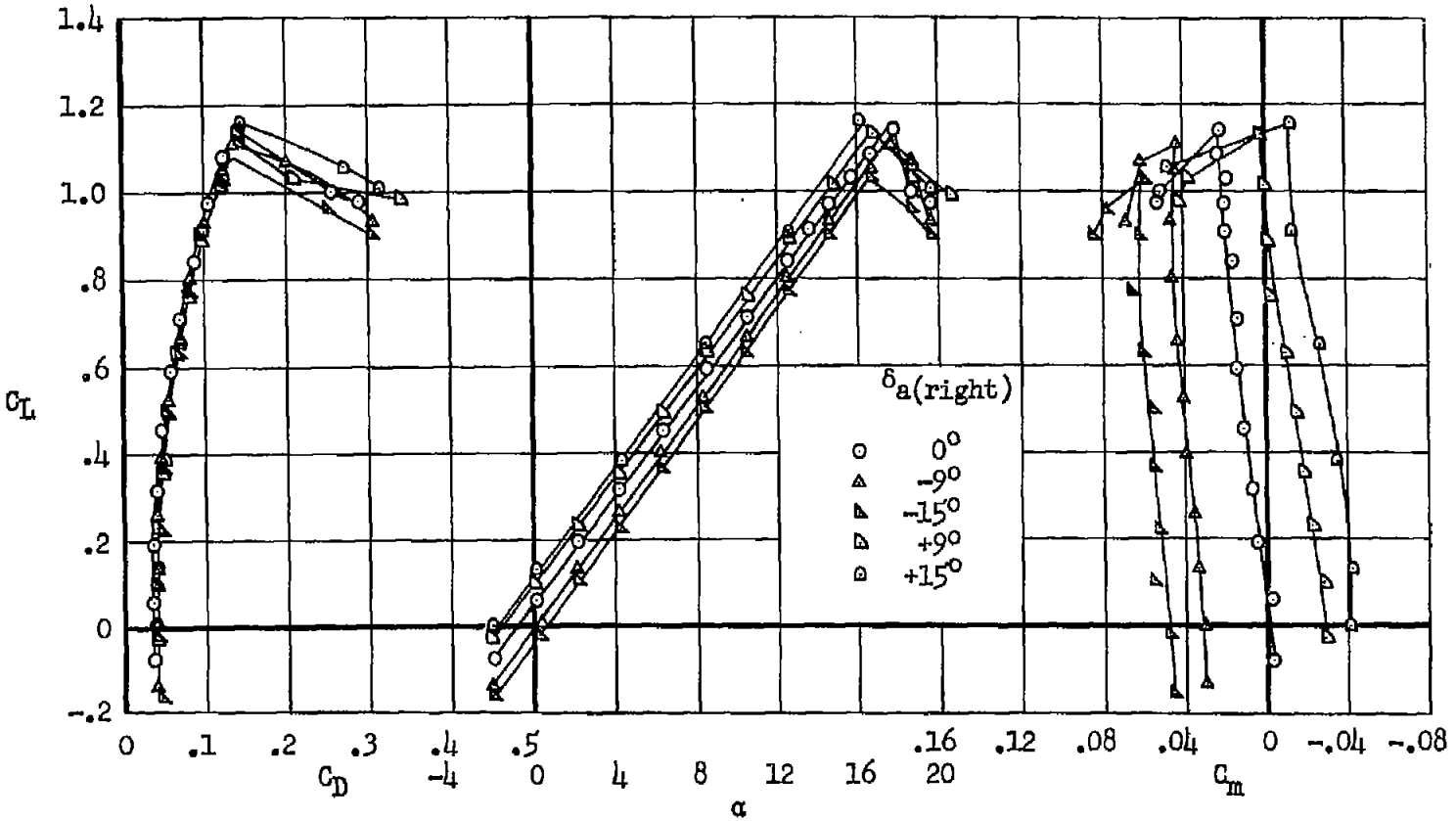

(a) Longitudinal characteristics.

Figure 8.- Effect of aileron deflection on the aerodynamic characteristics of the airplane; $\delta_f = 0°$, blowing off.

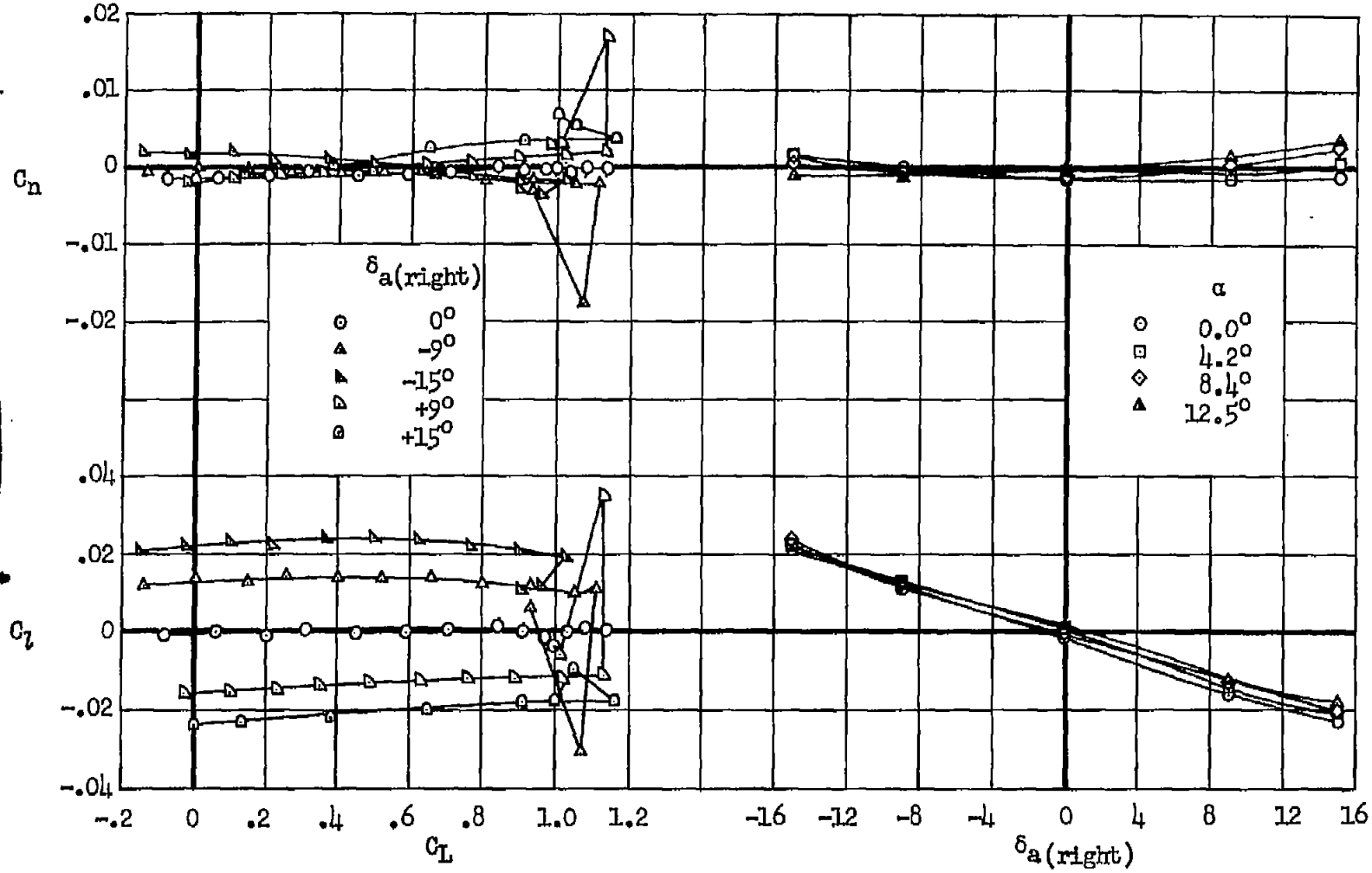

(b) Lateral characteristics.

Figure 8.- Concluded.

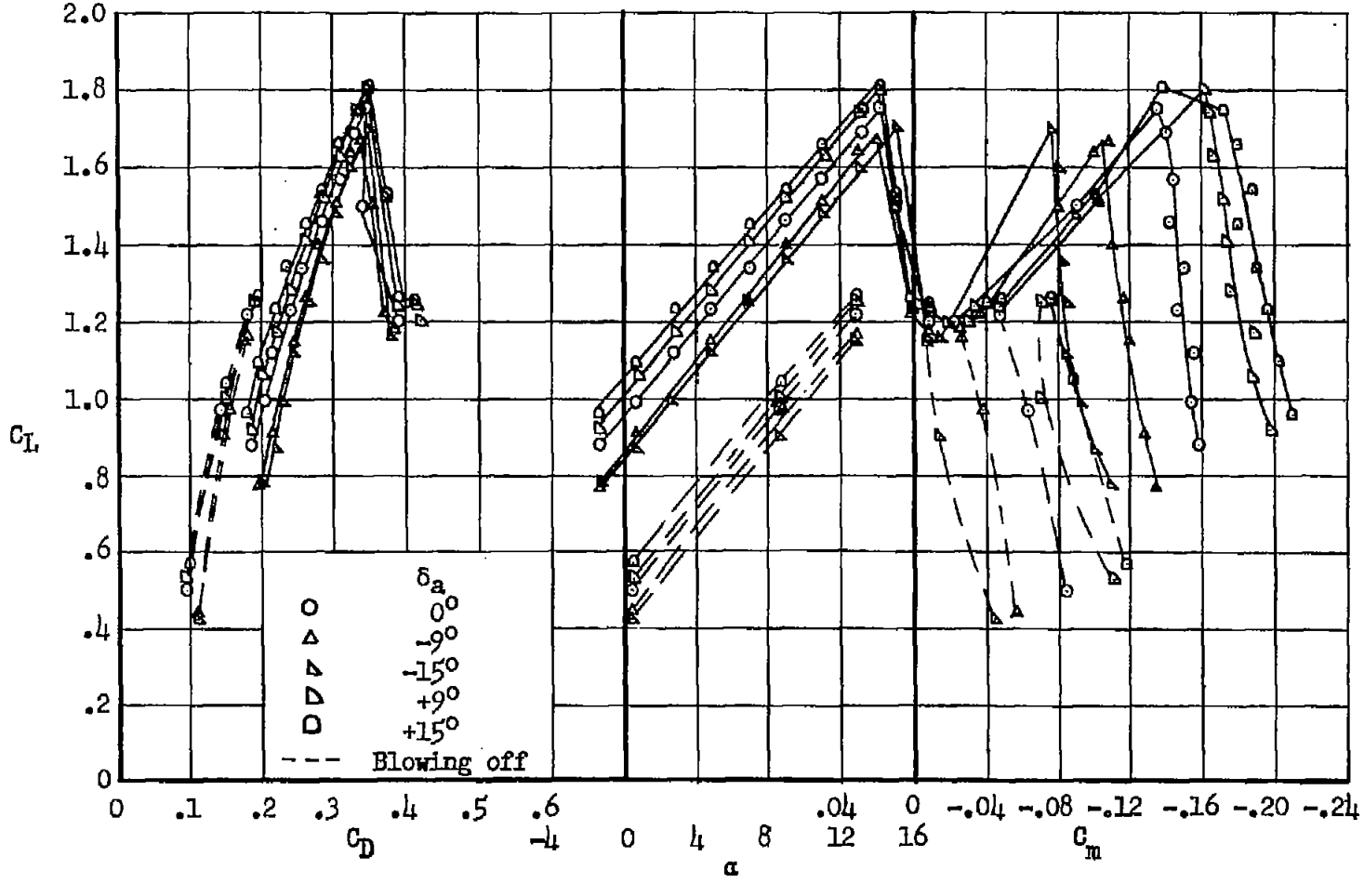

(a) Longitudinal characteristics.

Figure 9.- Effect of aileron deflection on the aerodynamic characteristics of the airplane; $\delta_f = 60°$, $C_\mu = 0.017$.

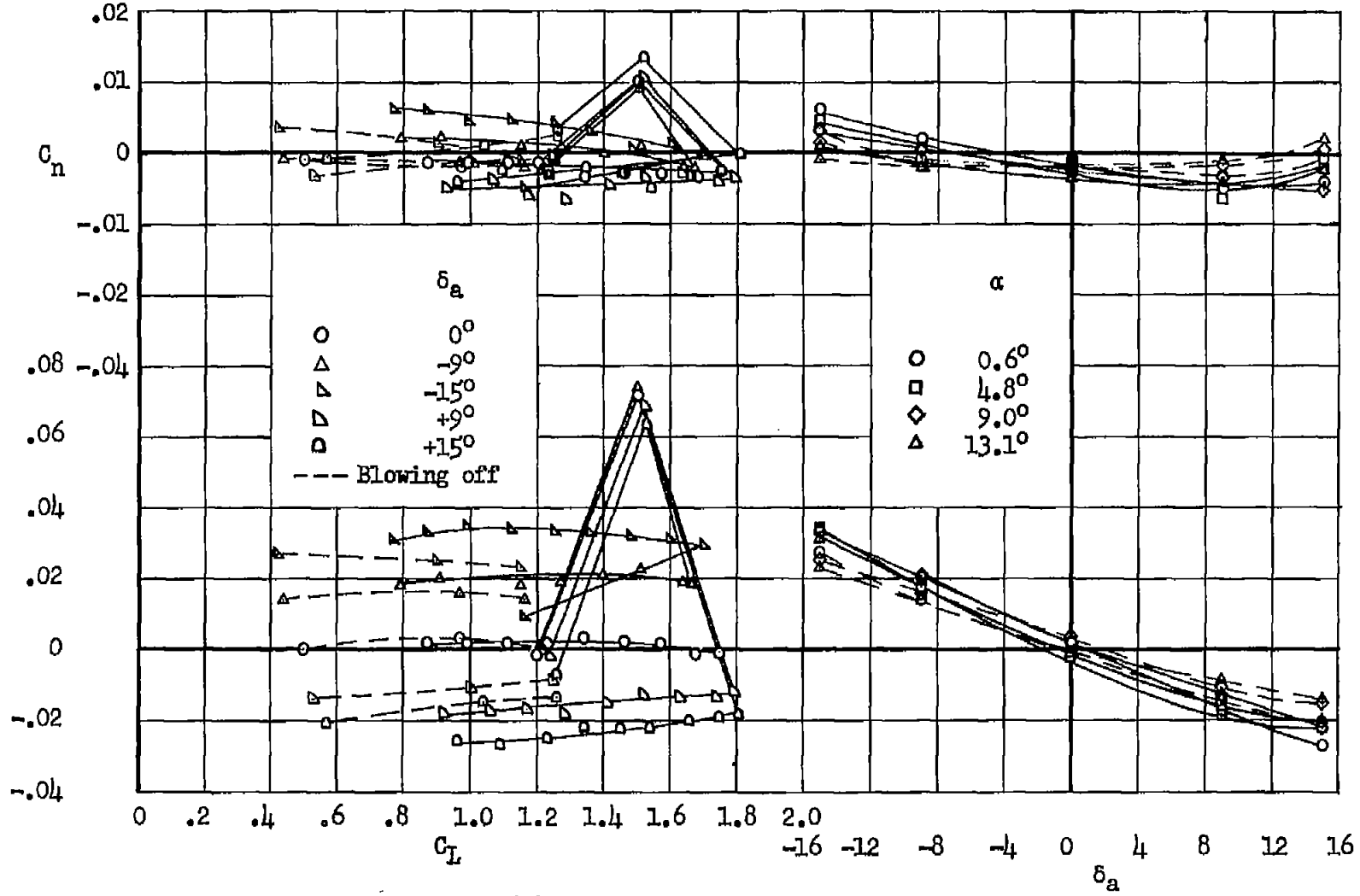

(b) Lateral characteristics.

Figure 9.- Concluded.

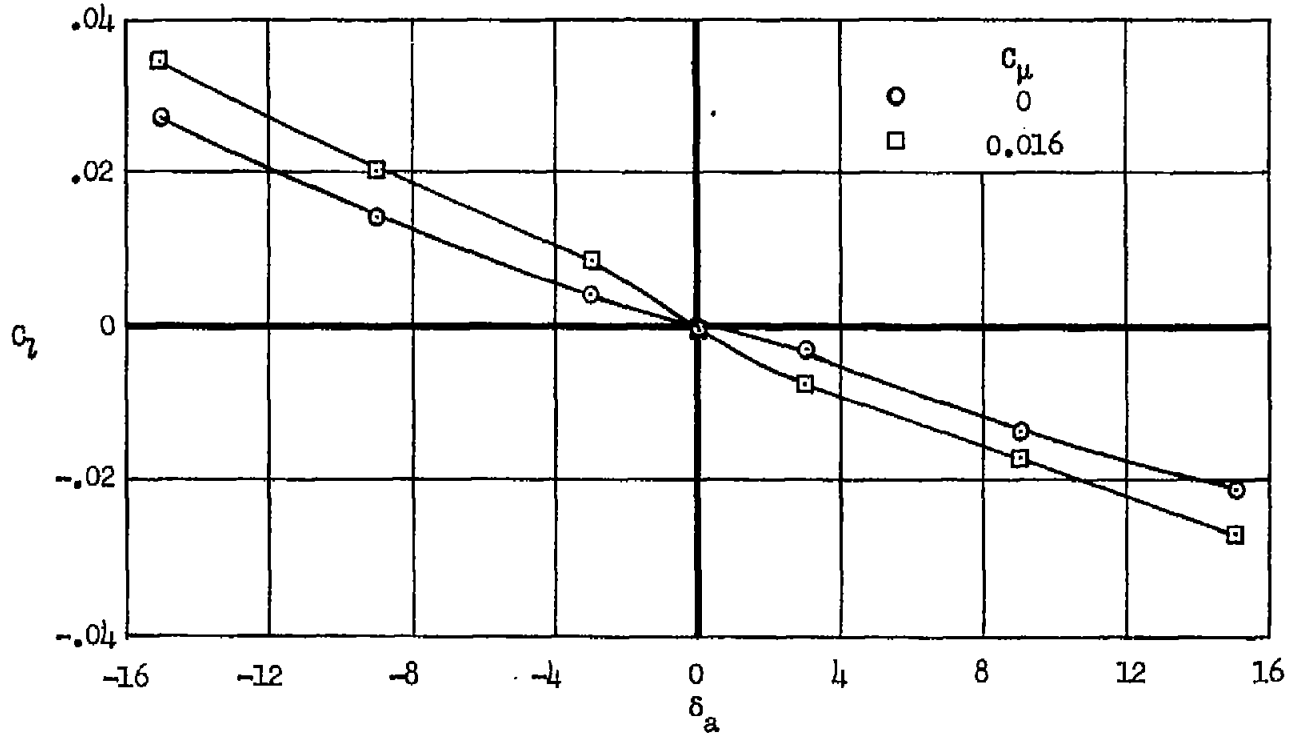

Figure 10.- Comparison of aileron effectiveness without and with flap blowing; $\delta_f = 60^\circ$.

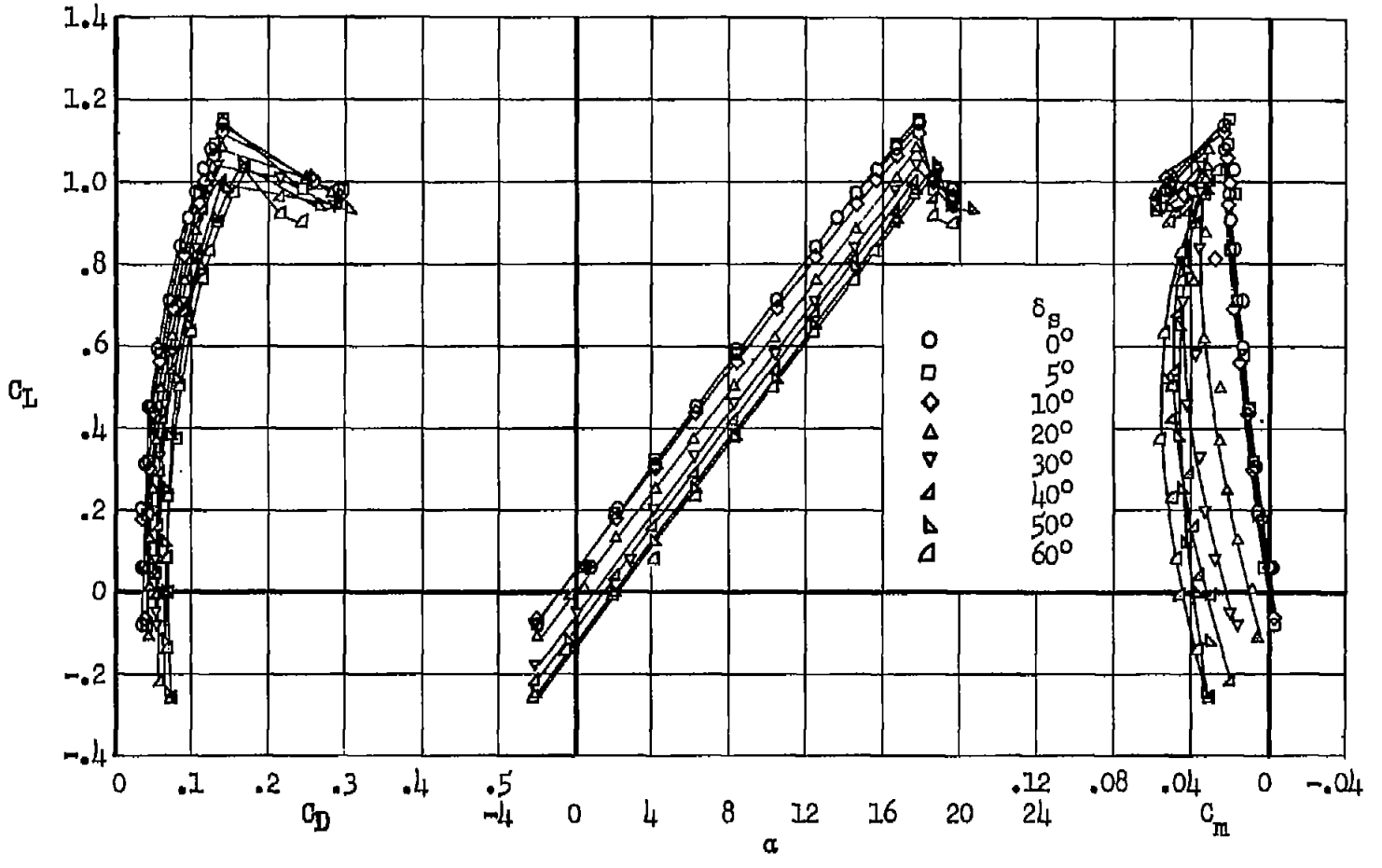

(a) Longitudinal characteristics.

Figure 11.- Effect of spoiler deflection on the aerodynamic characteristics of the airplane; 0.87-semispan spoiler, $\delta_f = 0^\circ$.

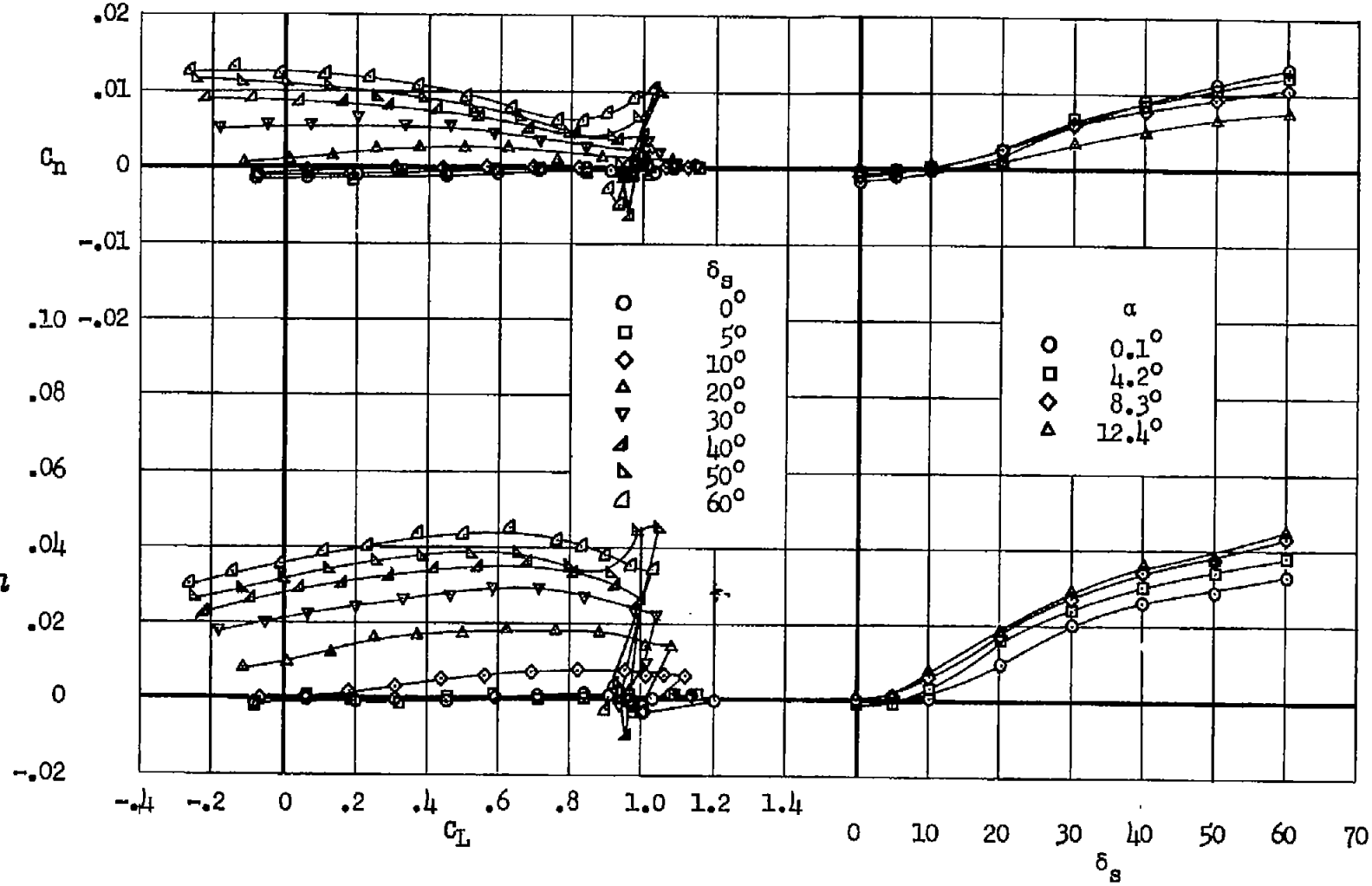

(b) Lateral characteristics.

Figure 11.- Concluded.

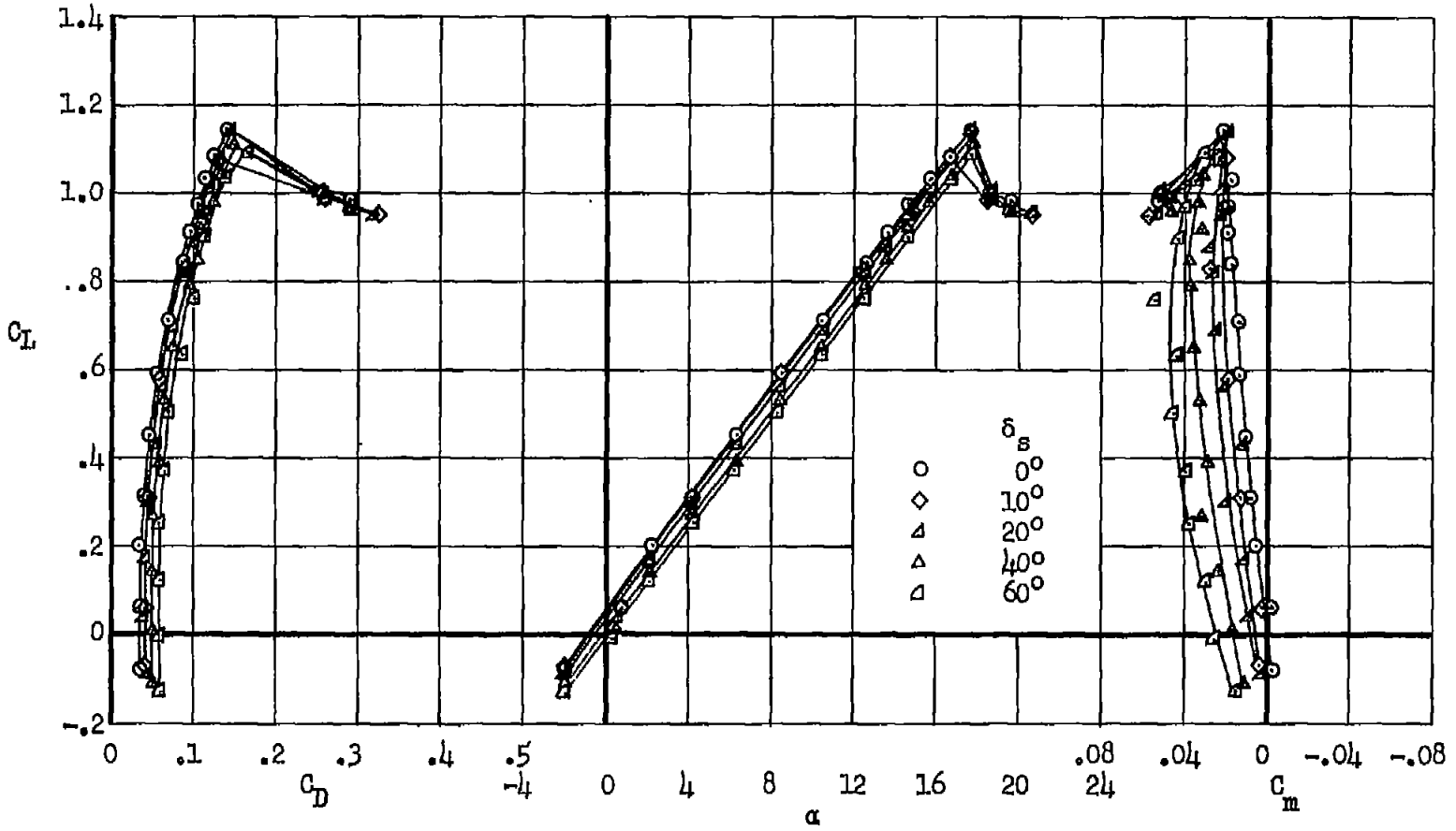

(a) Longitudinal characteristics.

Figure 12.- Effect of spoiler deflection on the aerodynamic characteristics of the airplane; 0.55-semispan spoiler, $\delta_f = 0°$.

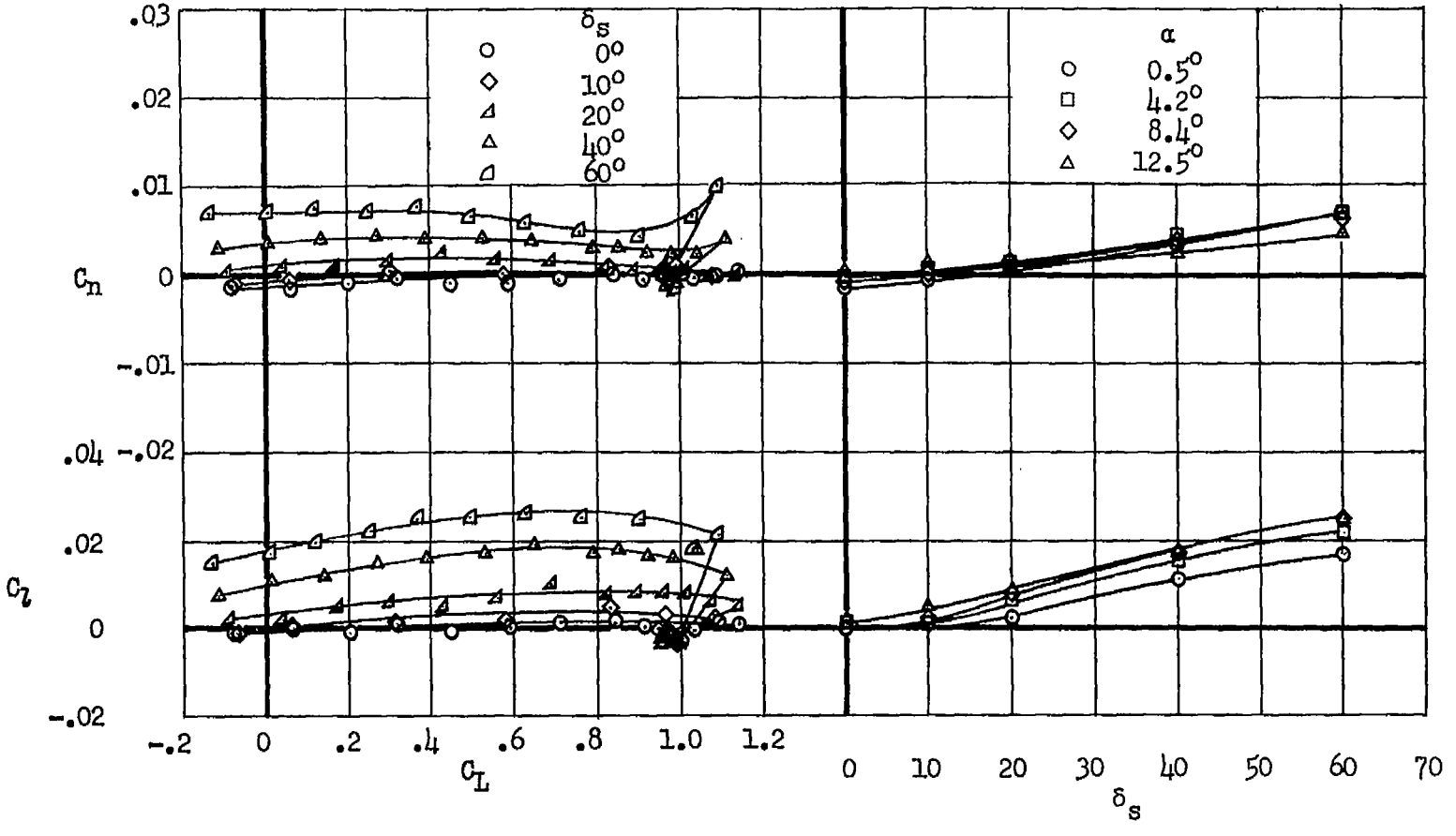

(b) Lateral characteristics.

Figure 12.- Concluded.

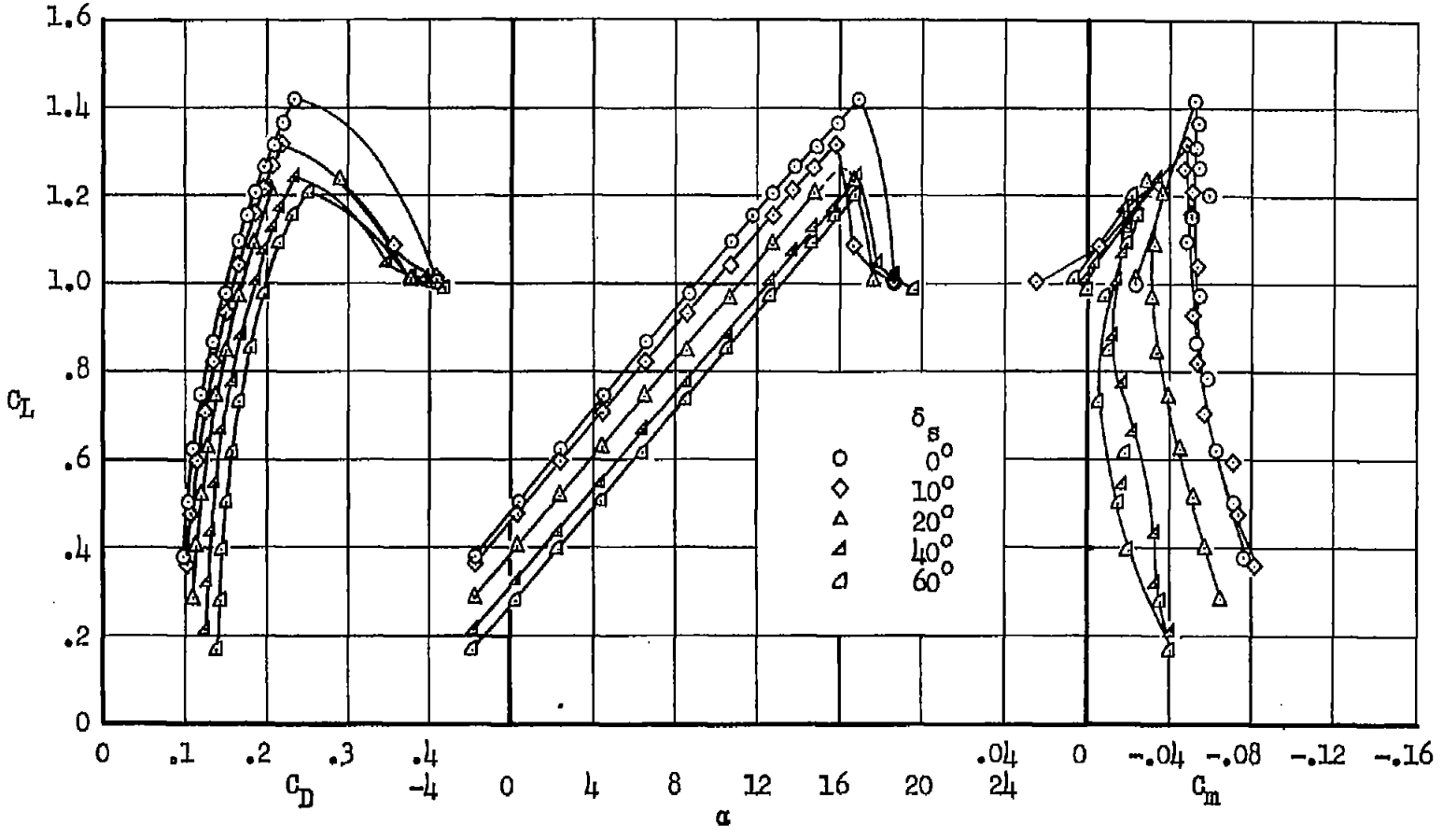

(a) Longitudinal characteristics.

Figure 13.- Effects of spoiler deflection on the aerodynamic characteristics of the airplane; 0.87-semispan spoiler, $\delta_f = 60^\circ$, $C_\mu = 0$.

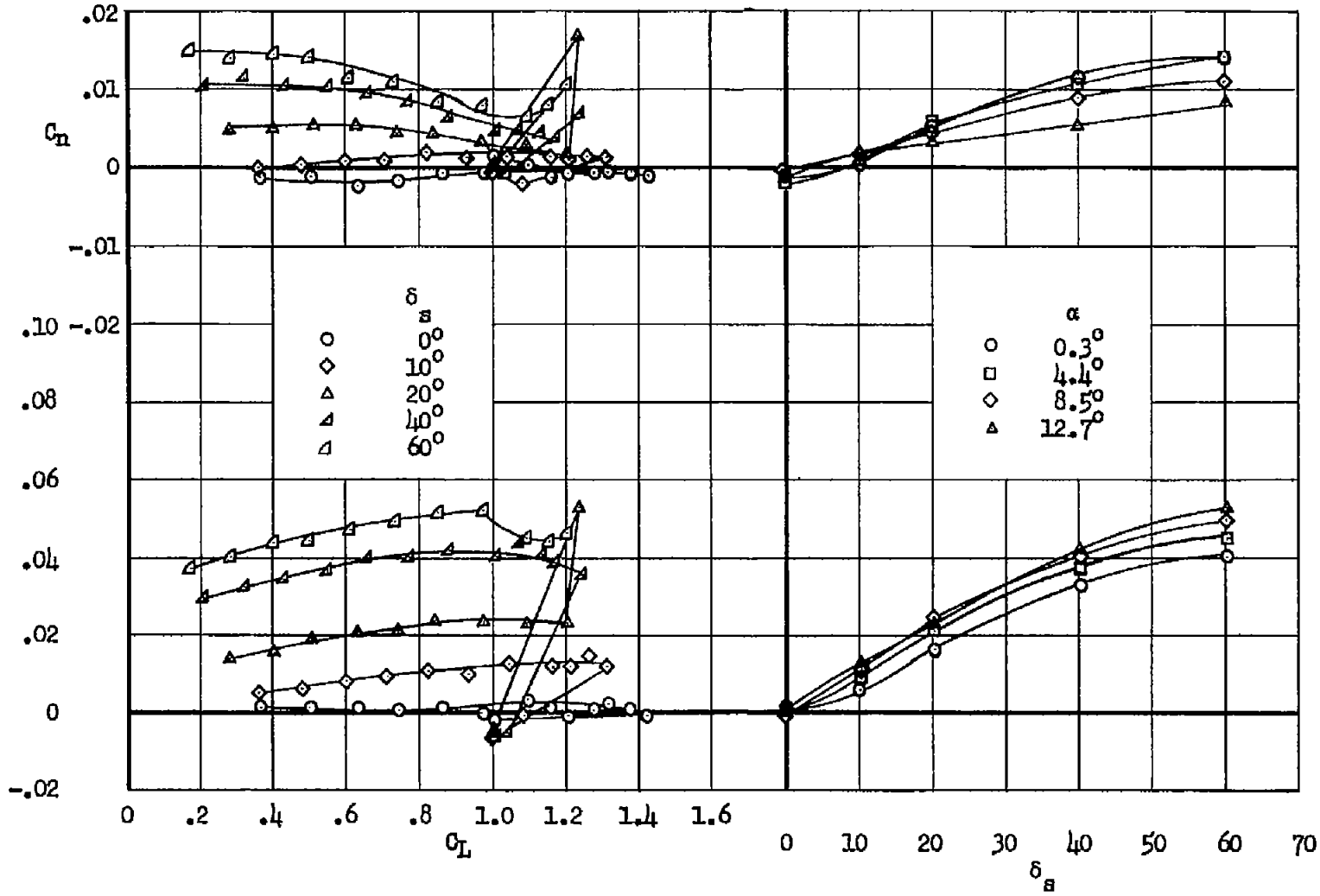

(b) Lateral characteristics.

Figure 13.- Concluded.

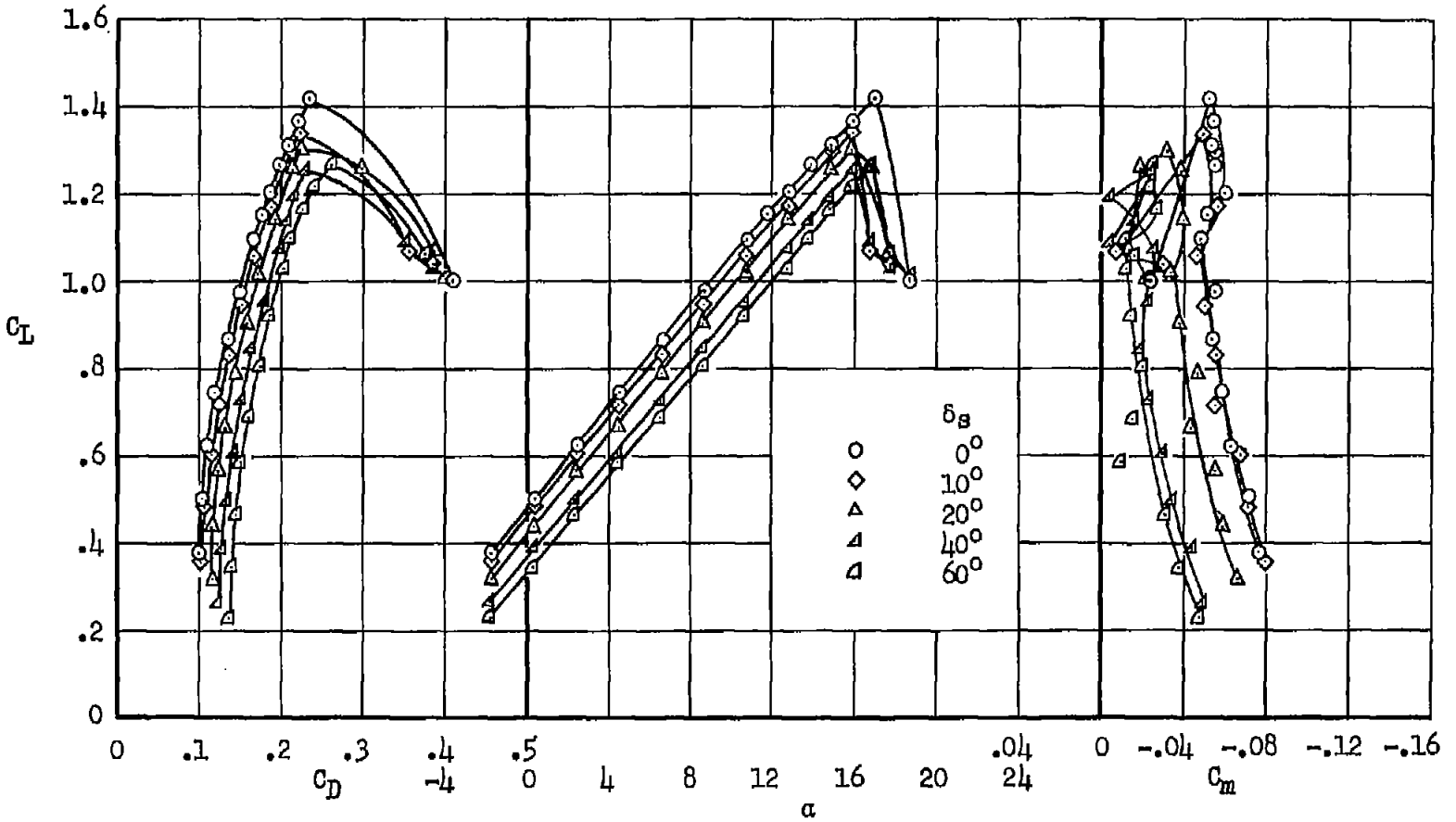

(a) Longitudinal characteristics.

Figure 14.- Effects of deflection on the aerodynamic characteristics of the airplane; 0.68-semispan spoiler, $\delta_f = 60^\circ$, $C_\mu = 0$.

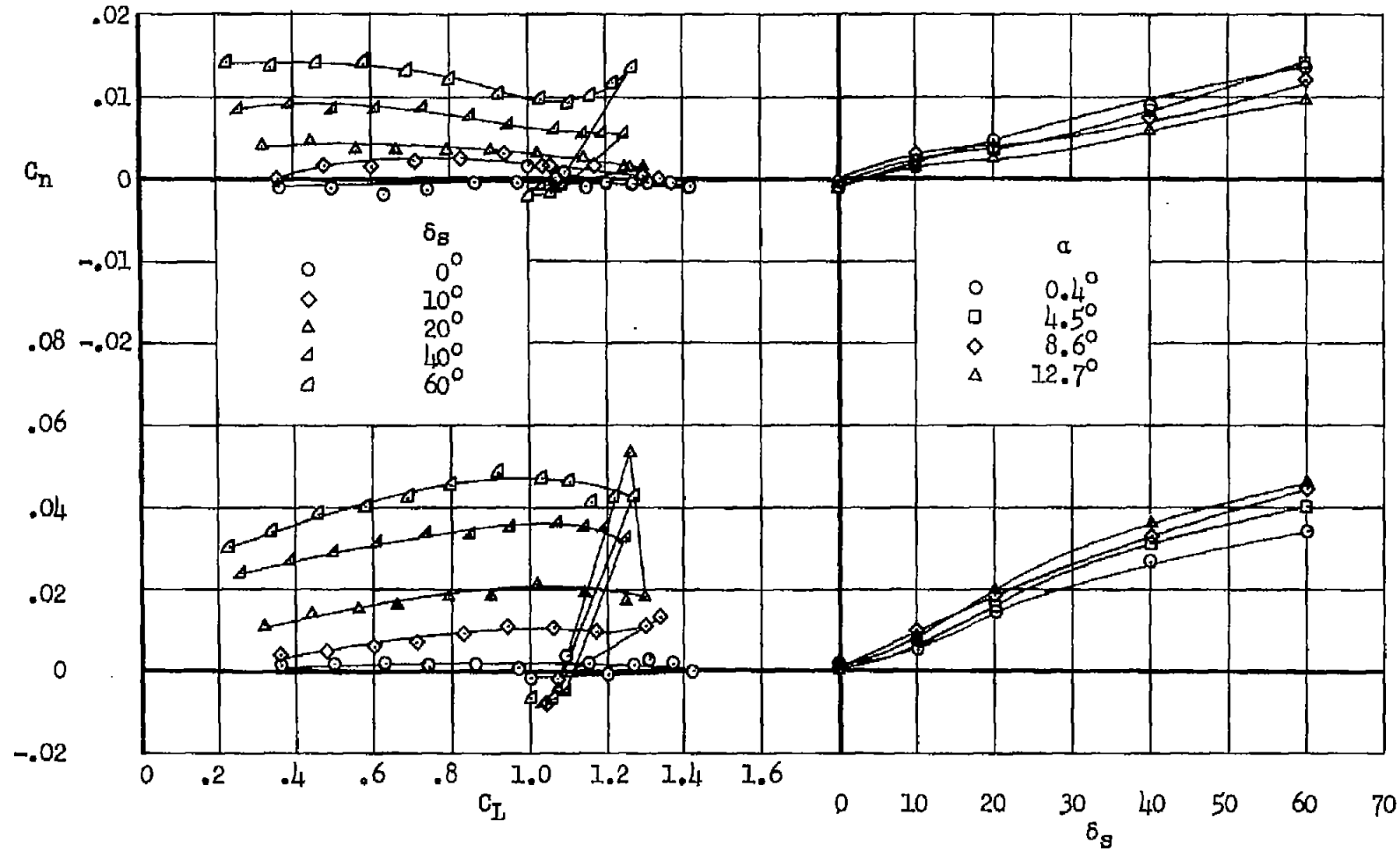

(b) Lateral characteristics.

Figure 14.- Concluded.

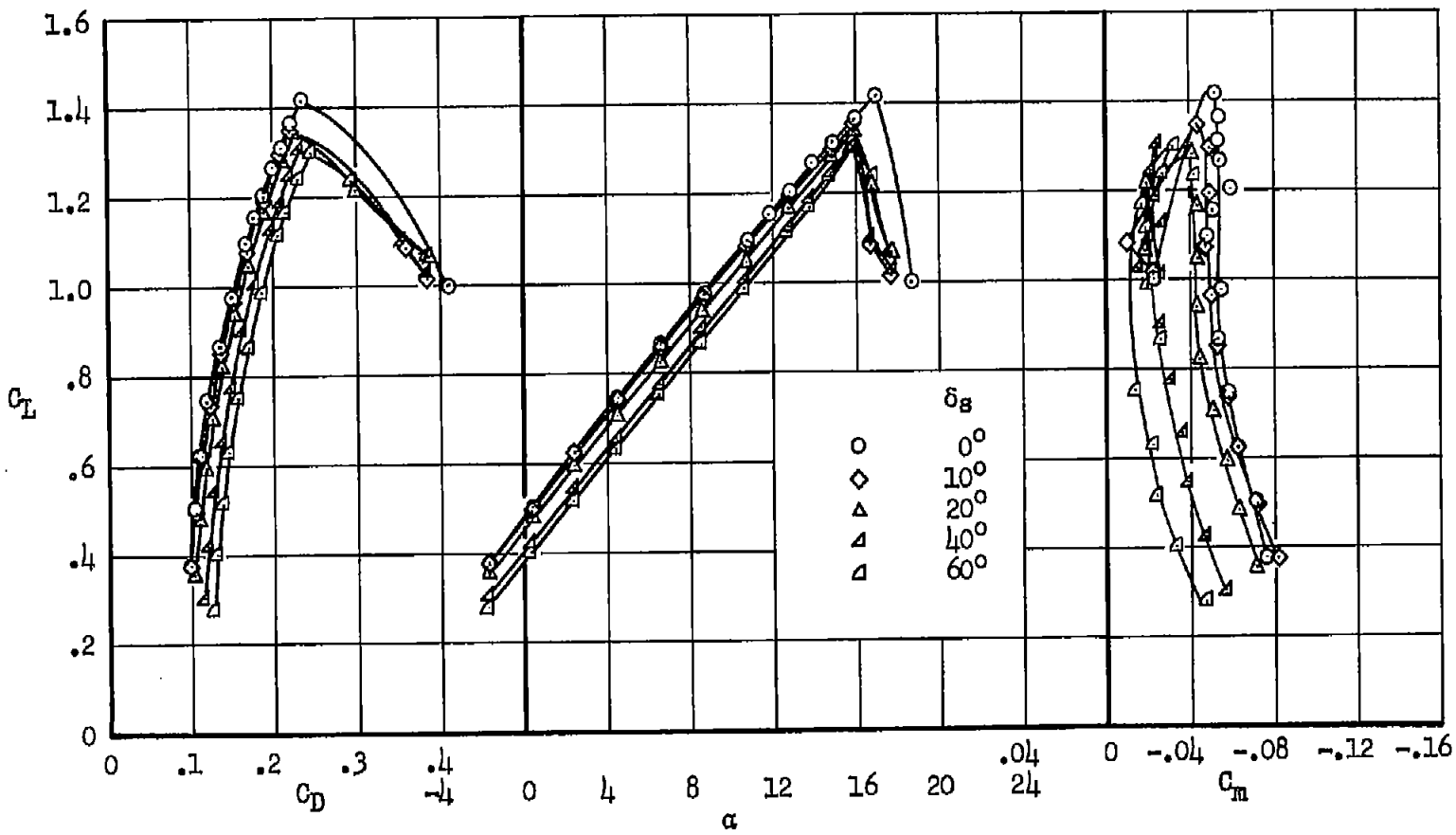

(a) Longitudinal characteristics.

Figure 15.- Effects of spoiler deflection on the aerodynamic characteristics of the airplane; 0.55-semispan spoiler, $\delta_f = 60°$, $C_\mu = 0$.

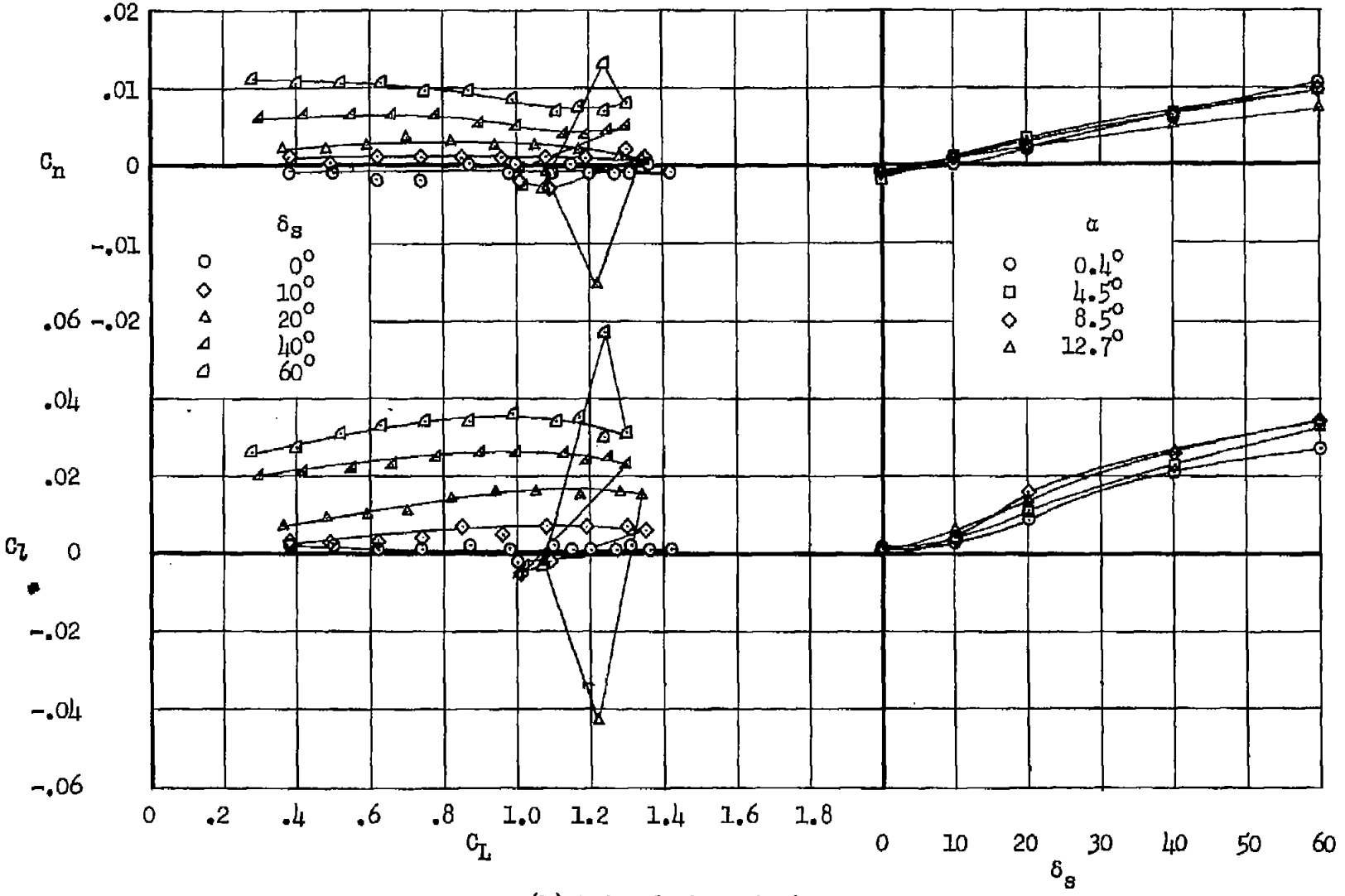

(b) Lateral characteristics.

Figure 15.- Concluded.

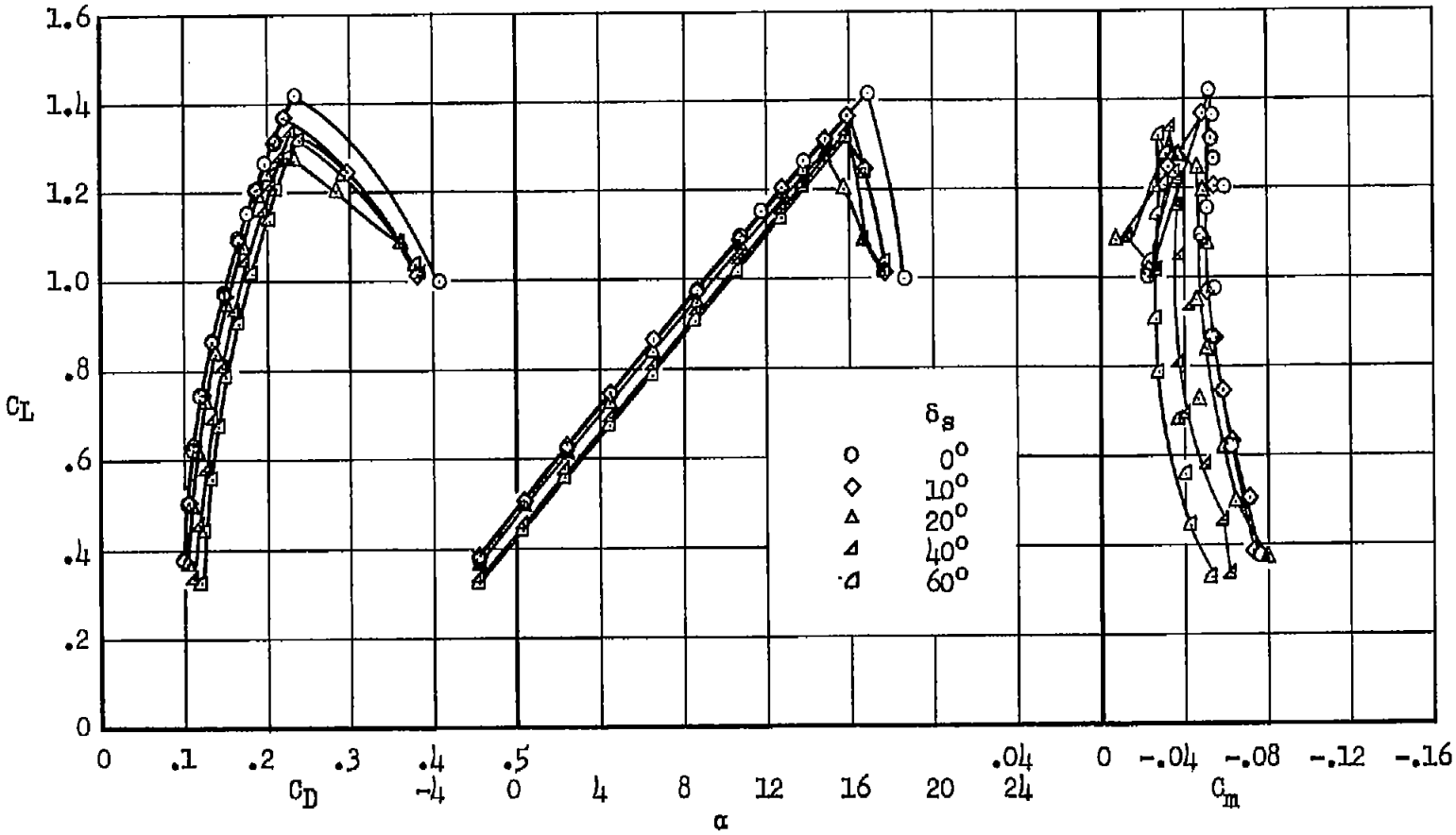

(a) Longitudinal characteristics.

Figure 16.- Effects of spoiler deflection on the aerodynamic characteristics of the airplane; 0.47-semispan spoiler, $\delta_f = 60°$, $C_\mu = 0$.

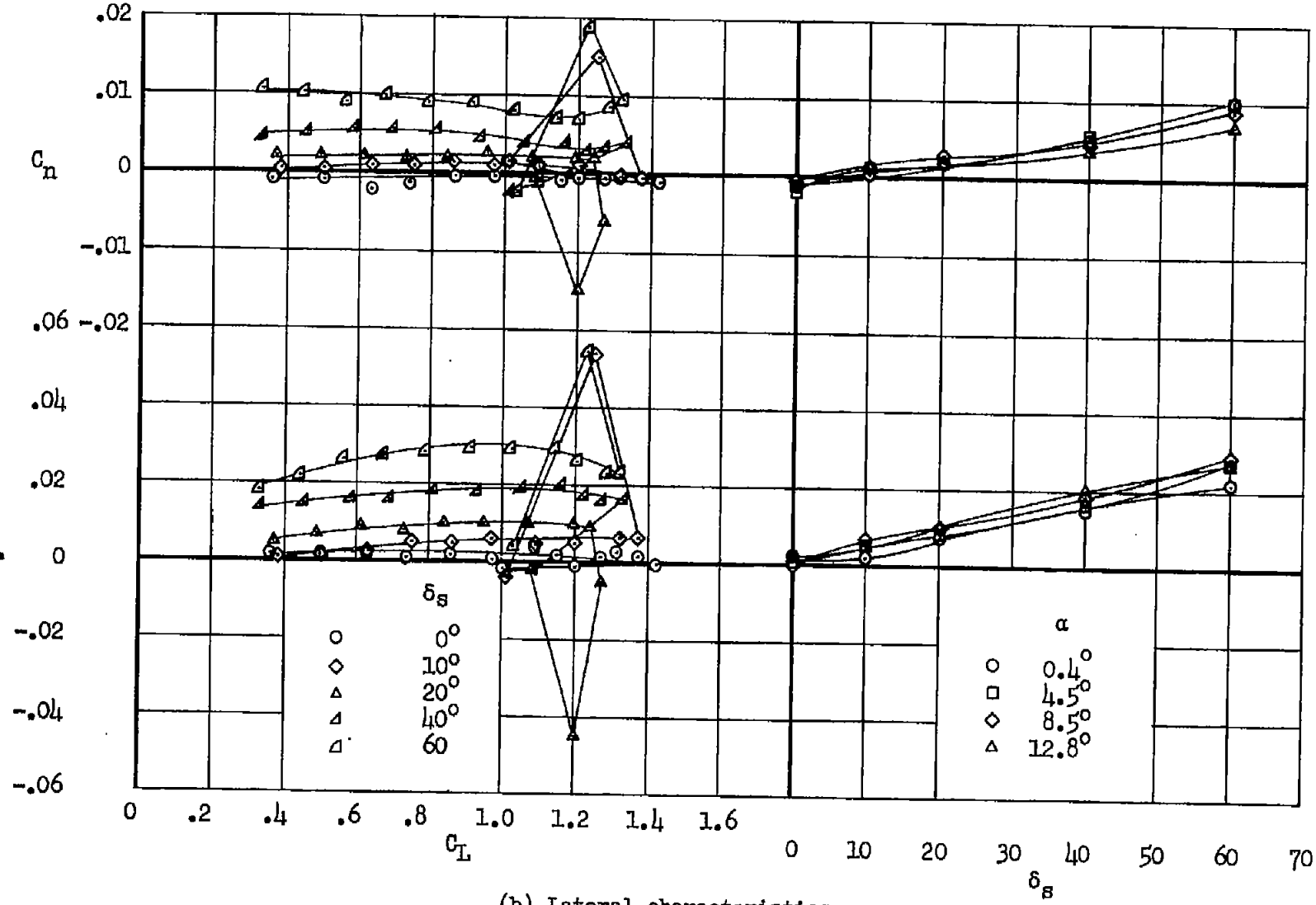

(b) Lateral characteristics.

Figure 16.- Concluded.

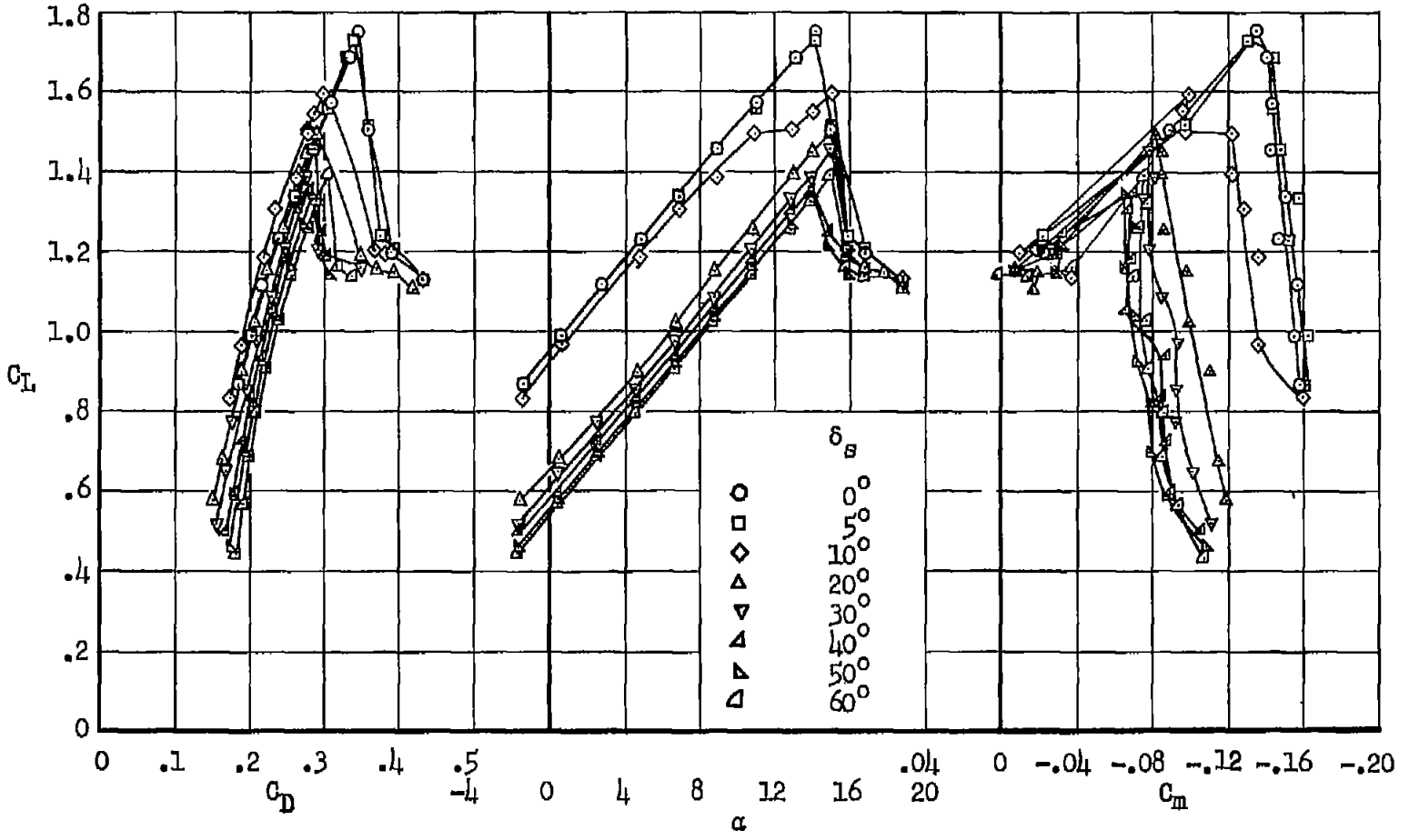

(a) Longitudinal characteristics.

Figure 17.- Effects of spoiler deflection on the aerodynamic characteristics of the airplane; 0.87-semispan spoiler, $\delta_f = 60^\circ$, $C_\mu = 0.017$.

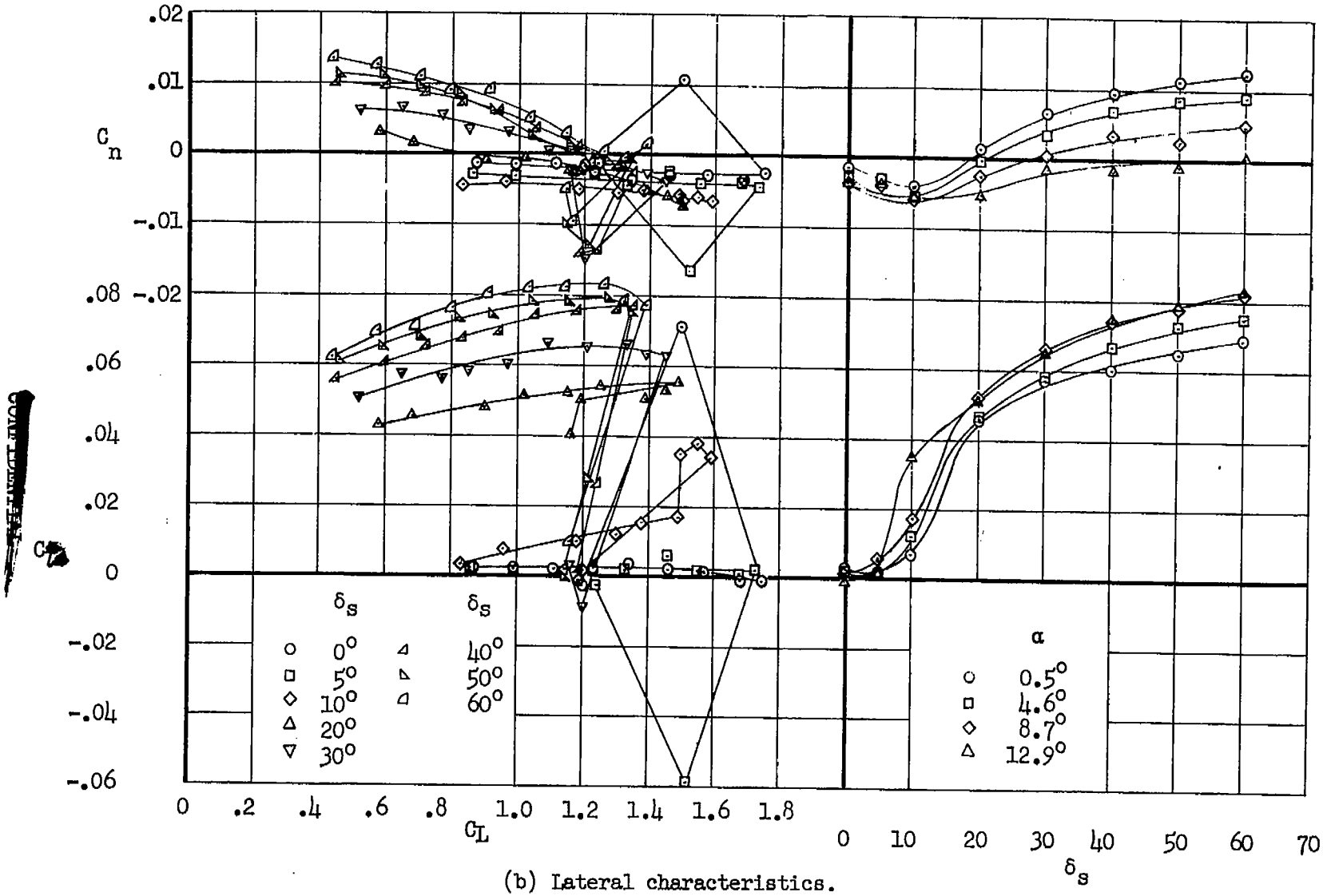

(b) Lateral characteristics.

Figure 17.- Concluded.

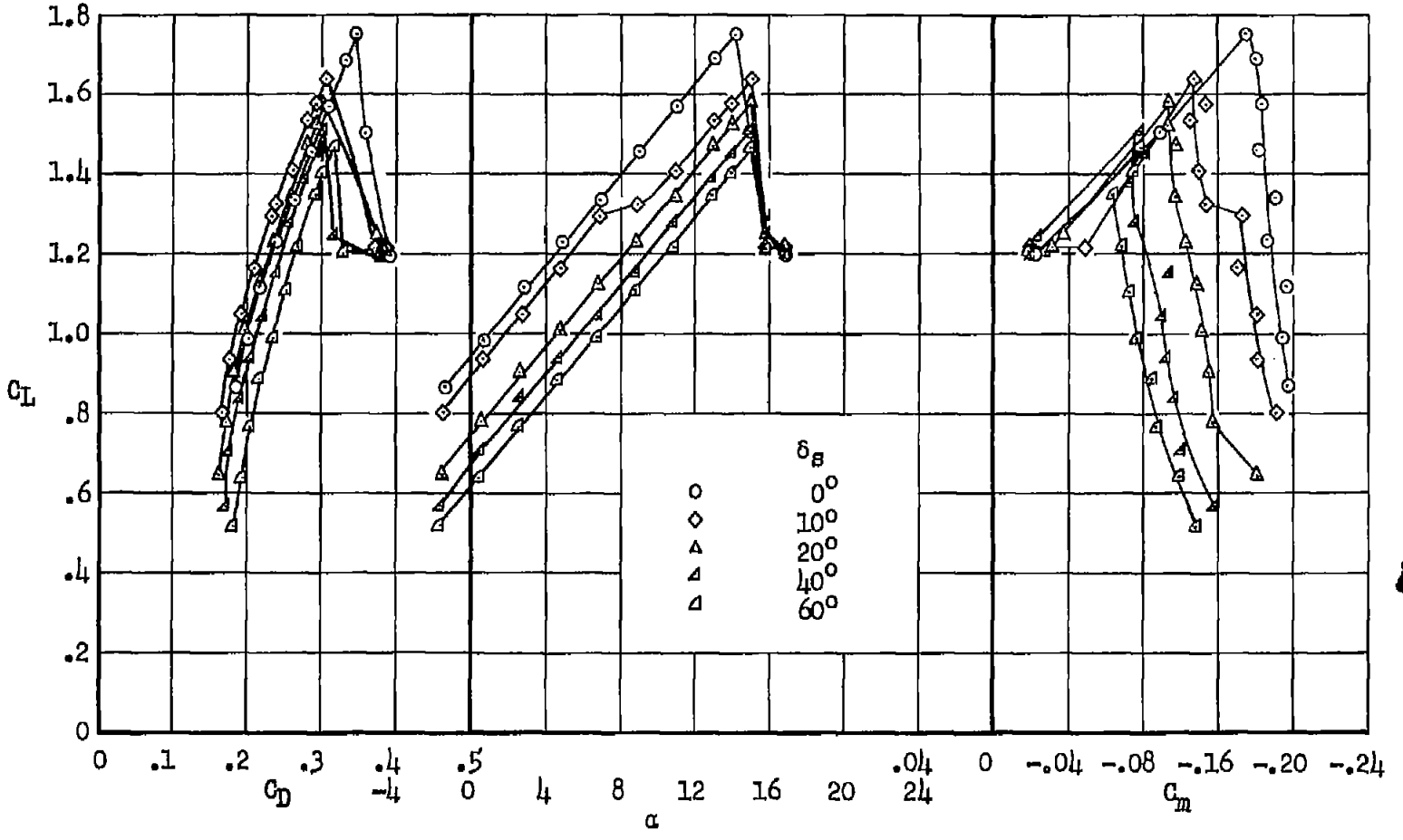

(a) Longitudinal characteristics.

Figure 18.- Effects of spoiler deflection on the aerodynamic characteristics of the airplane; 0.68-semispan spoiler, $\delta_f = 60^\circ$, $C_\mu = 0.017$.

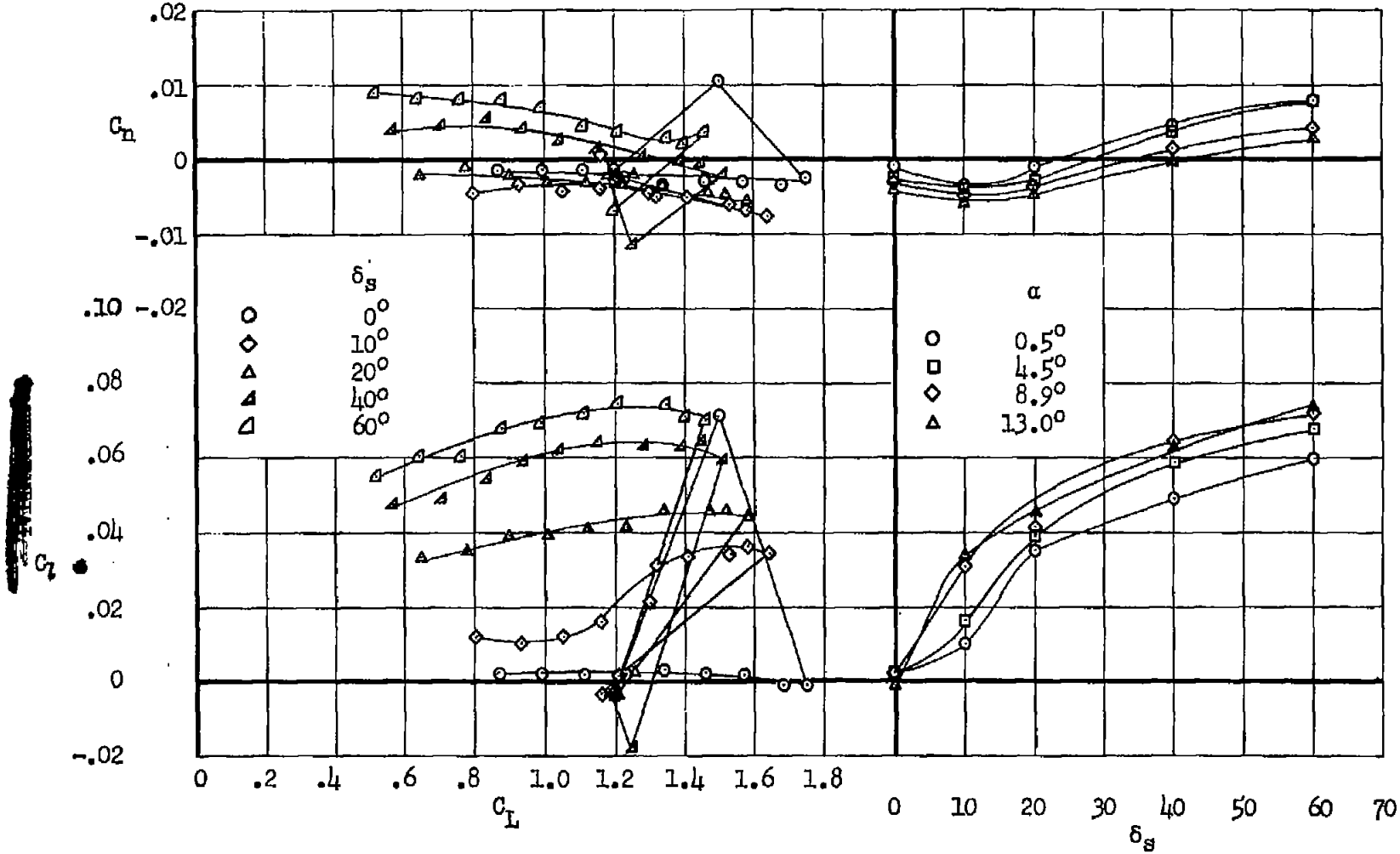

(b) Lateral characteristics.

Figure 18.- Concluded.

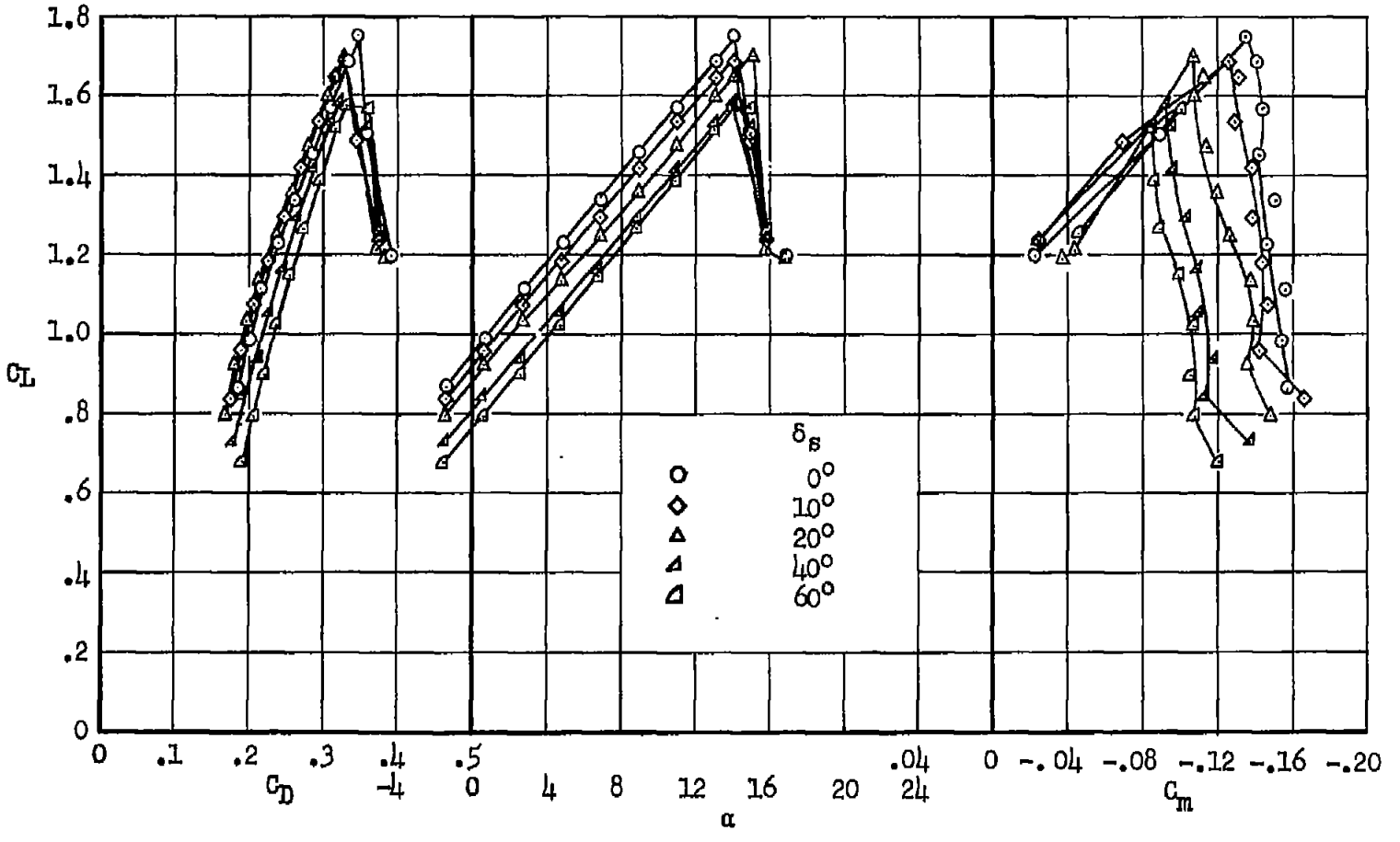

(a) Longitudinal characteristics.

Figure 19.- Effects of spoiler deflection on the aerodynamic characteristics of the airplane; 0.55-semispan spoiler, $\delta_f = 60°$, $C_\mu = 0.017$.

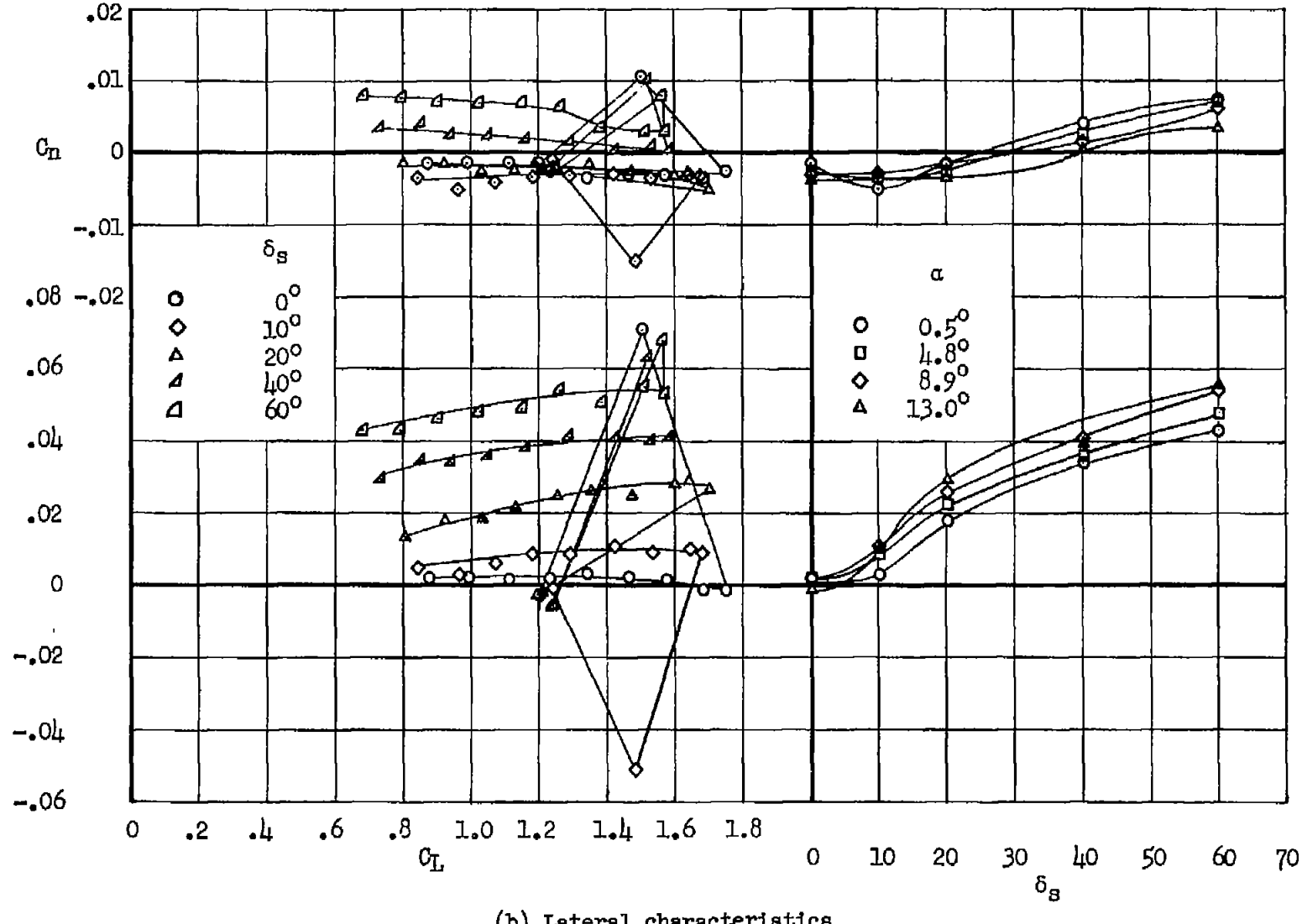

(b) Lateral characteristics.

Figure 19.- Concluded.

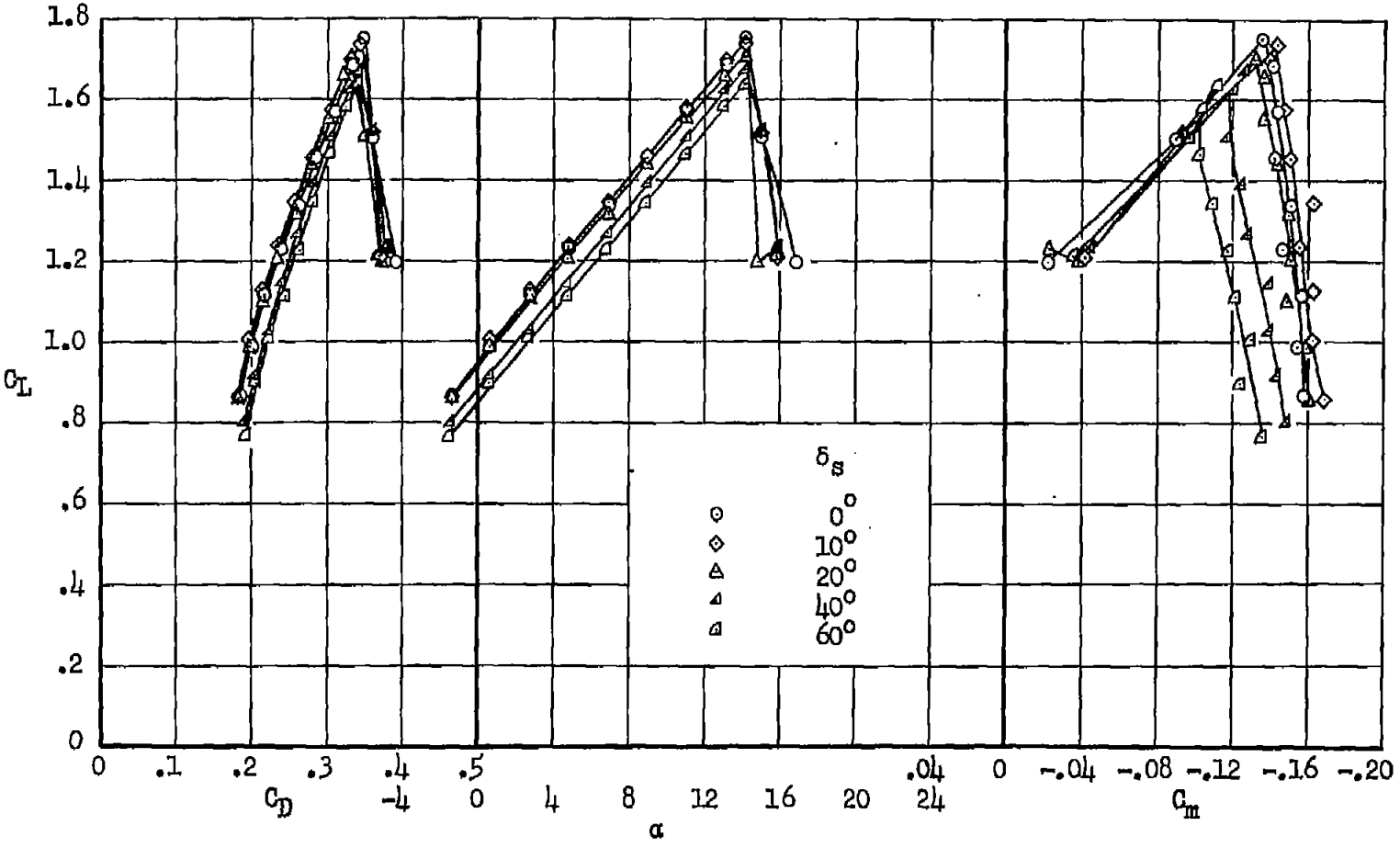

(a) Longitudinal characteristics.

Figure 20.- Effects of spoiler deflection on the aerodynamic characteristics of the airplane; 0.47-semispan spoiler, $\delta_f = 60°$, $C_\mu = 0.017$.

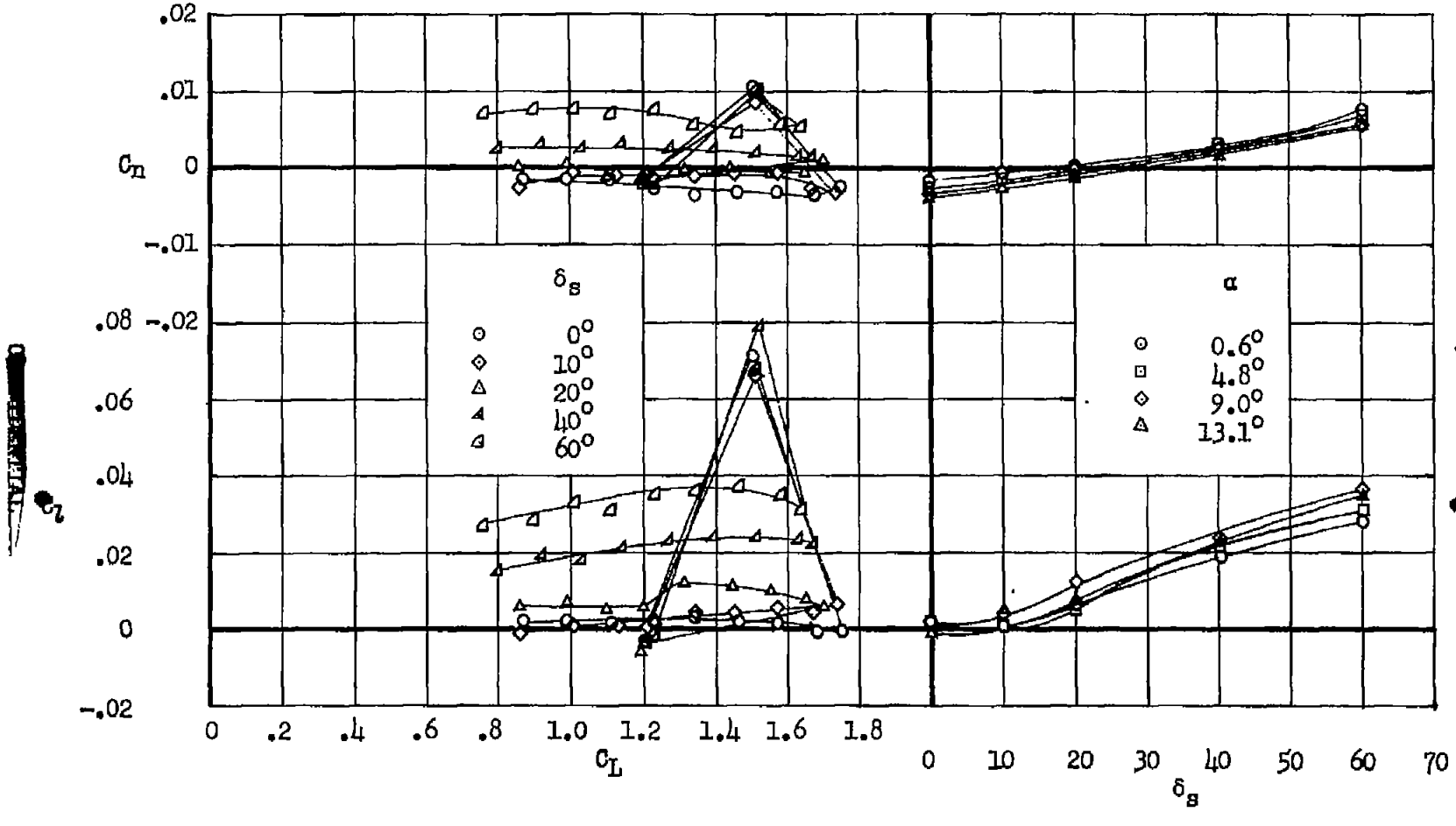

(b) Lateral characteristics.

Figure 20.- Concluded.

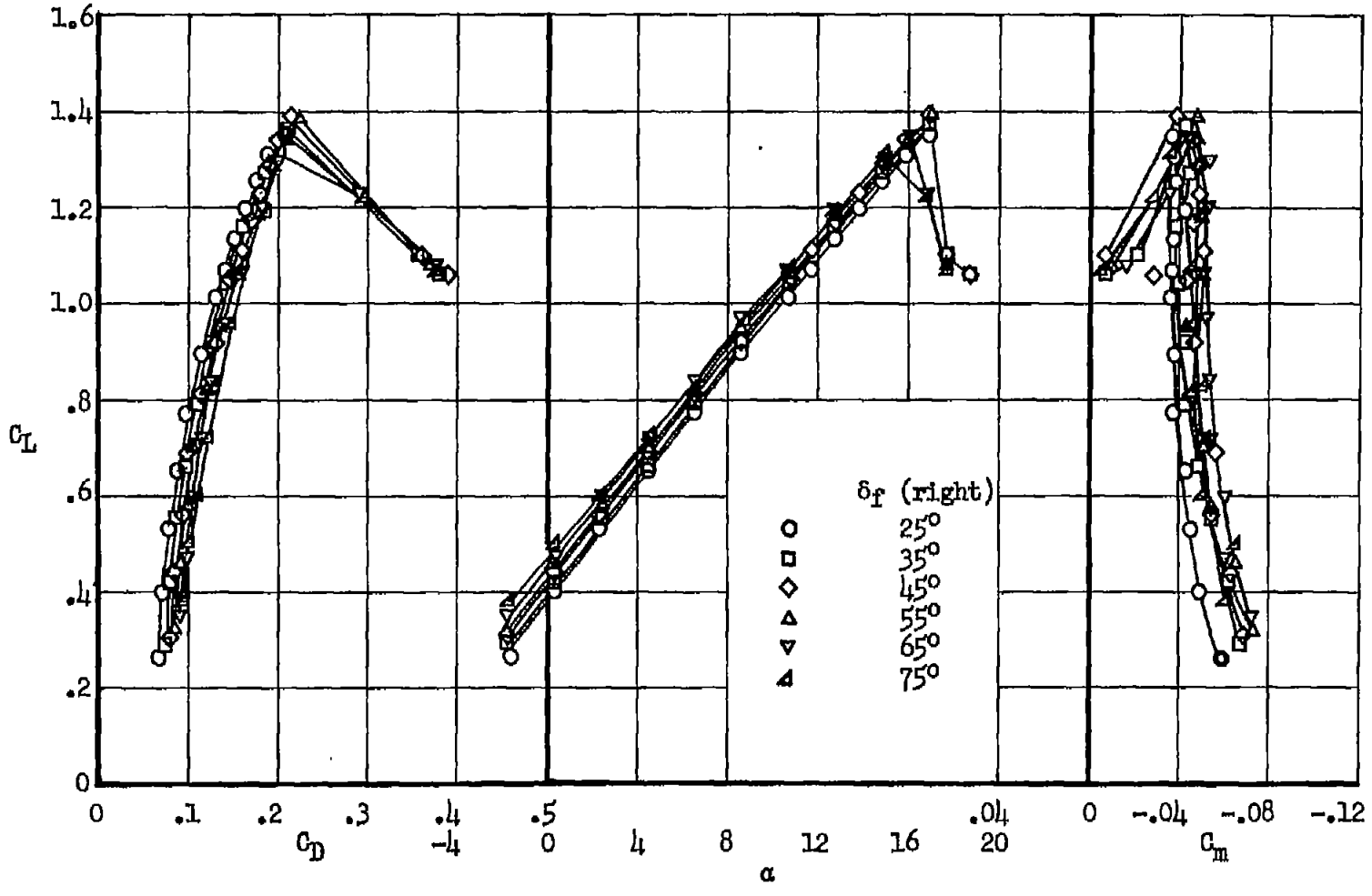

(a) Longitudinal characteristics.

Figure 21.- Effect of differentially deflected flaps on the aerodynamic characteristics of the airplane; δ_f (left) = 45°, C_μ = 0.

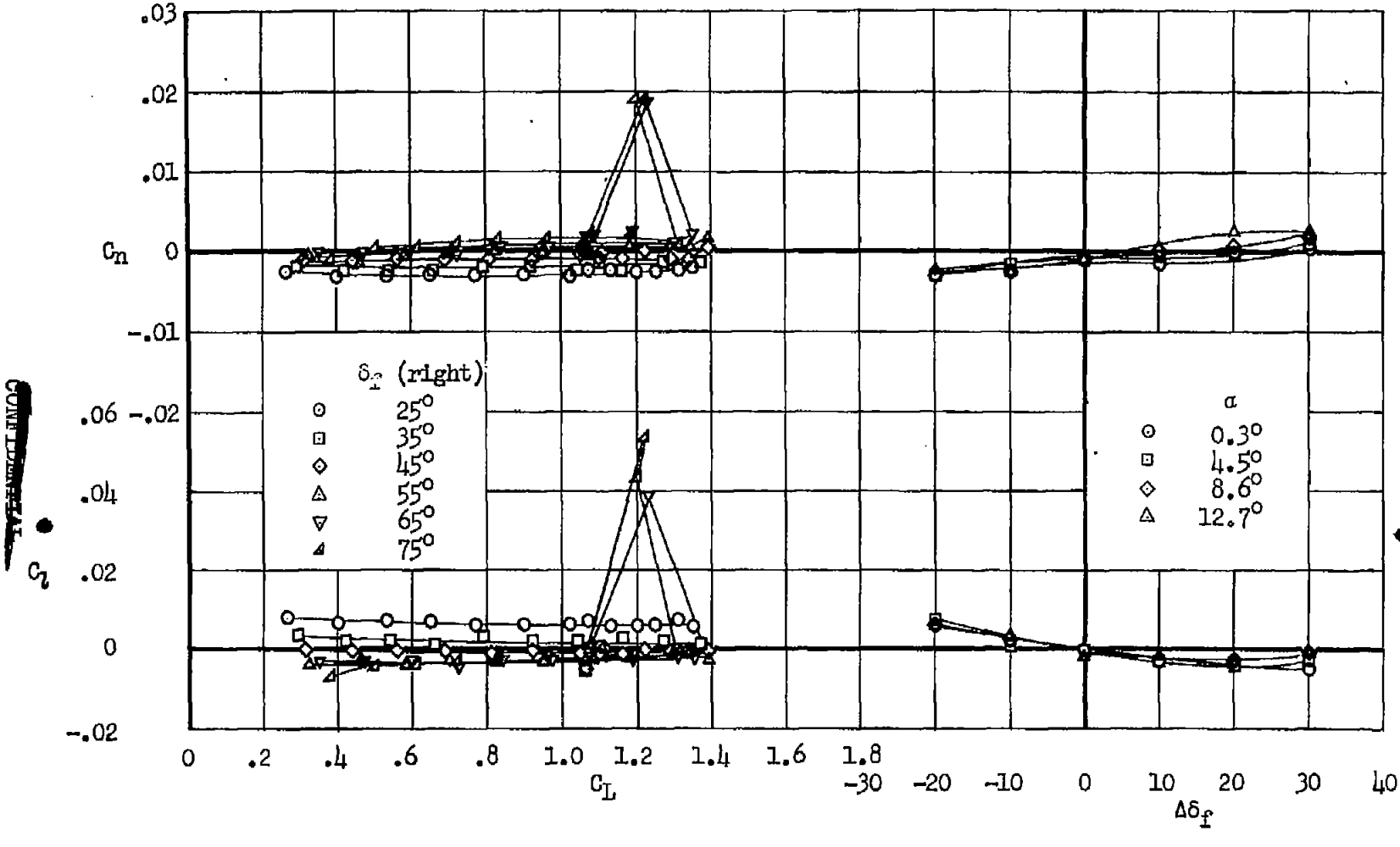

(b) Lateral characteristics.

Figure 21.- Concluded.

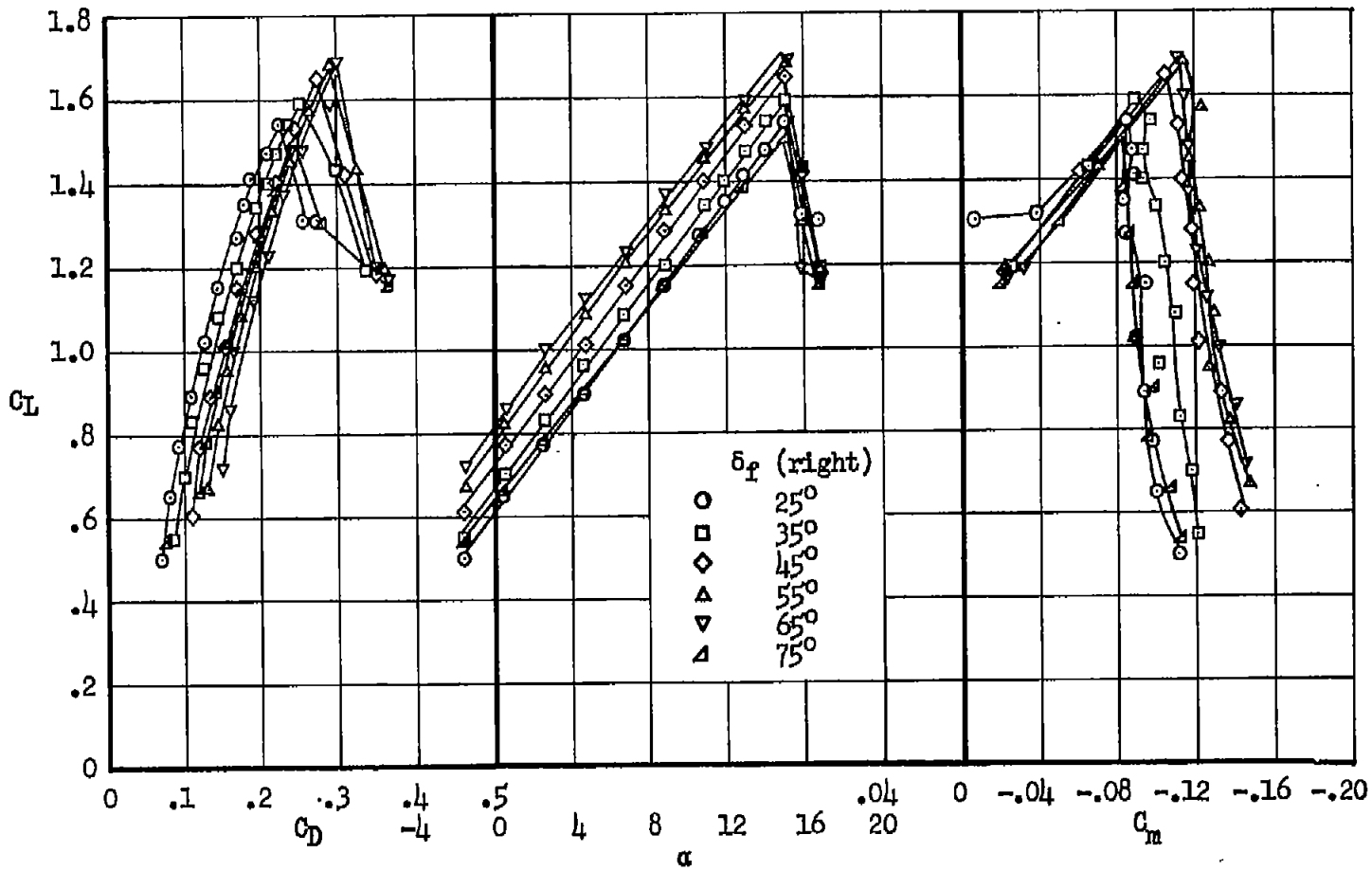

(a) Longitudinal characteristics.

Figure 22.- Effect of differentially deflected flaps on the aerodynamic characteristics of the airplane; δ_f (left) = 45°, $C_{\mu_R} = C_{\mu_L}$, $C_{\mu_R} + C_{\mu_L} = 0.012$, $\varphi = 22.5°$.

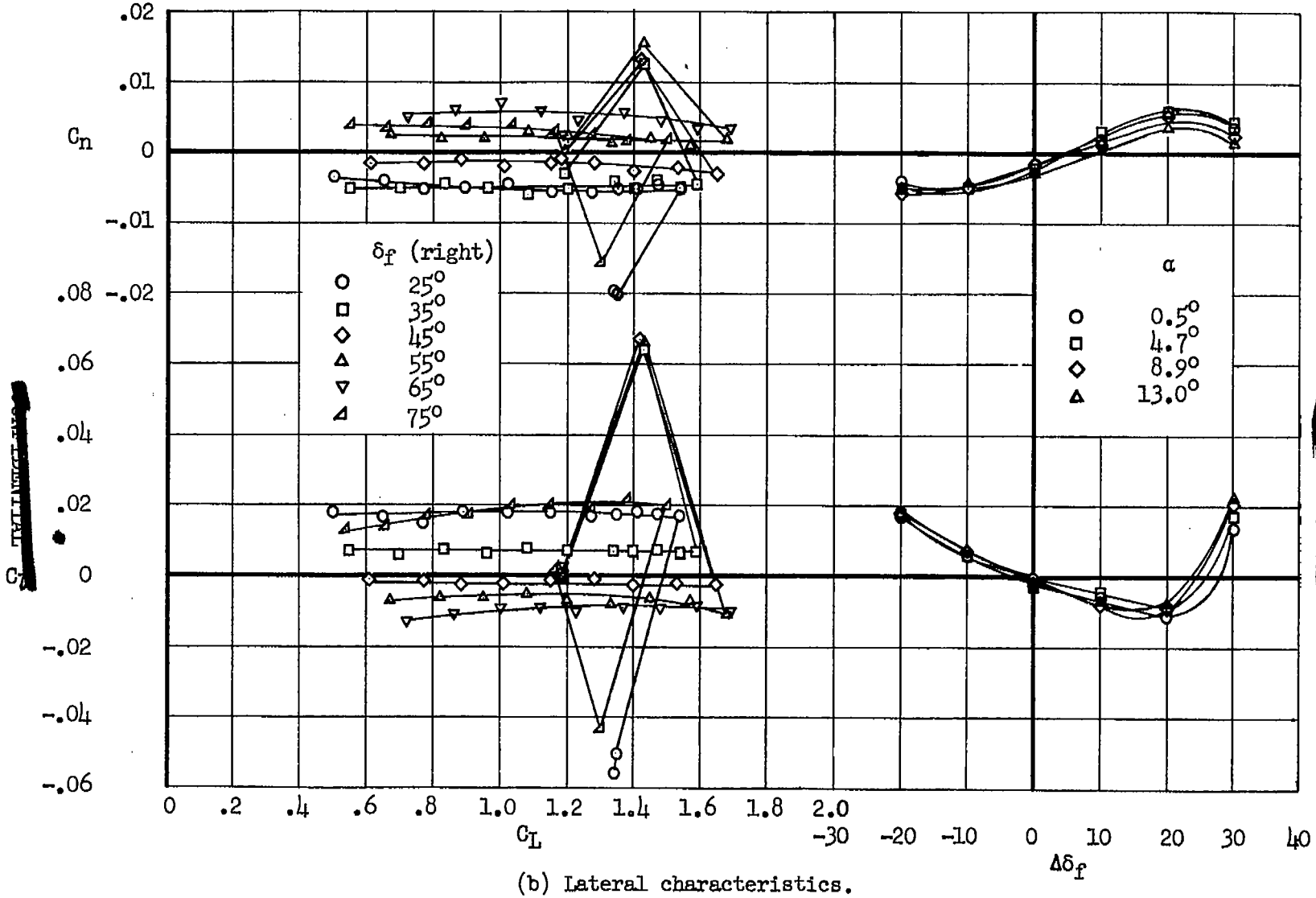

(b) Lateral characteristics.

Figure 22.- Concluded.

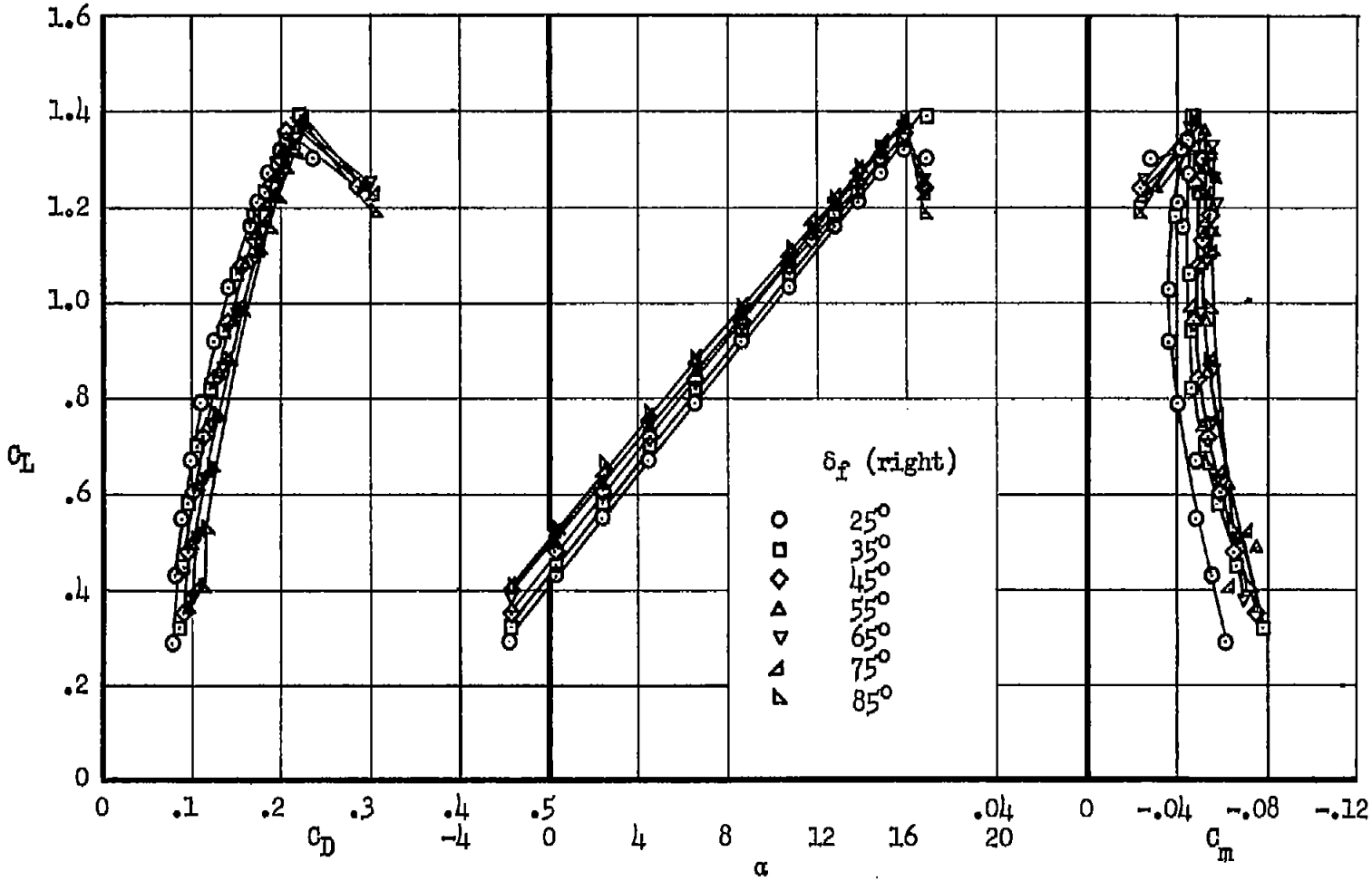

(a) Longitudinal characteristics.

Figure 23.- Effect of differentially deflected flaps on the aerodynamic characteristics of the airplane; δ_f (left) = 60°, C_μ = 0.

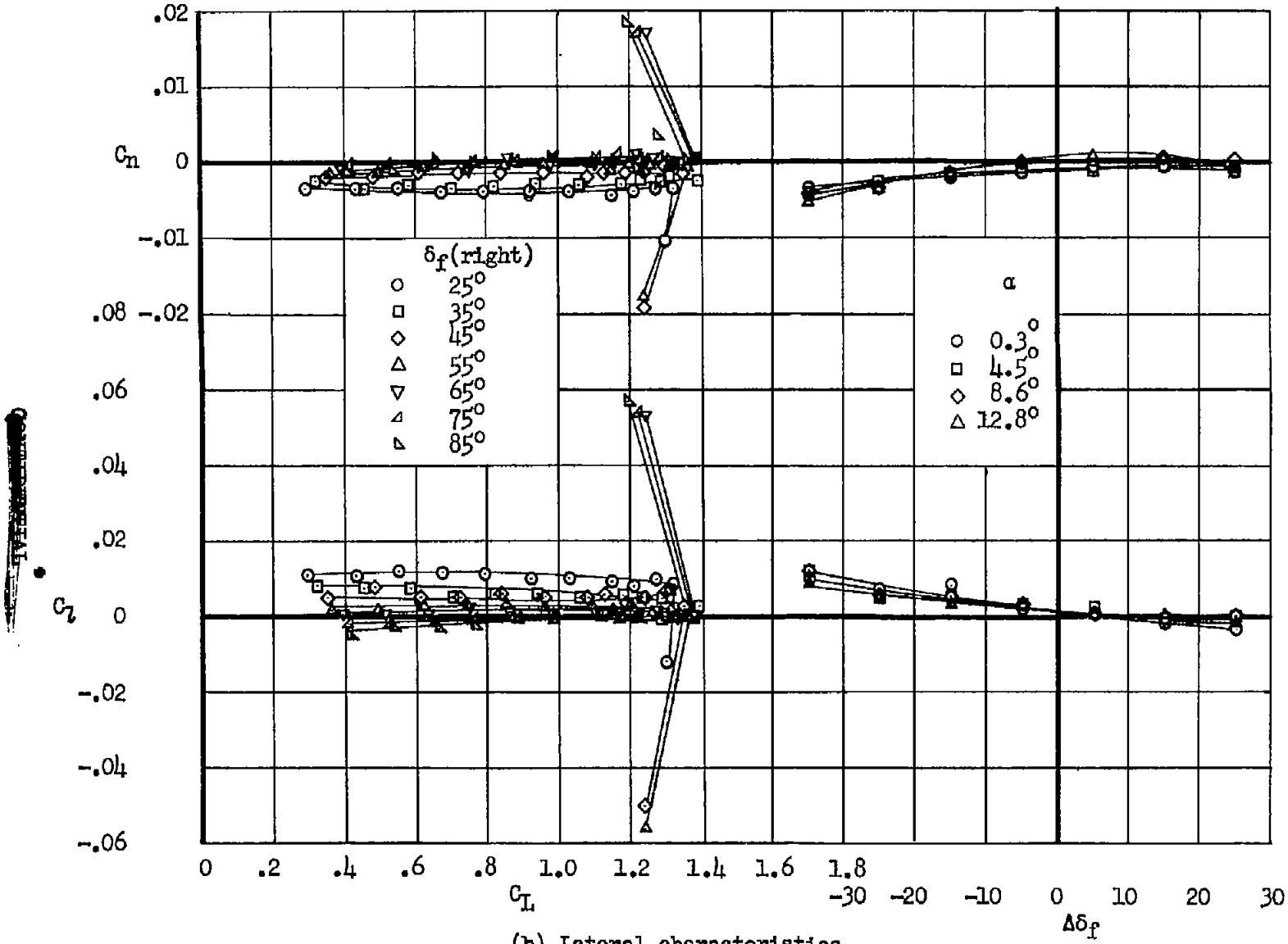

(b) Lateral characteristics.

Figure 23.- Concluded.

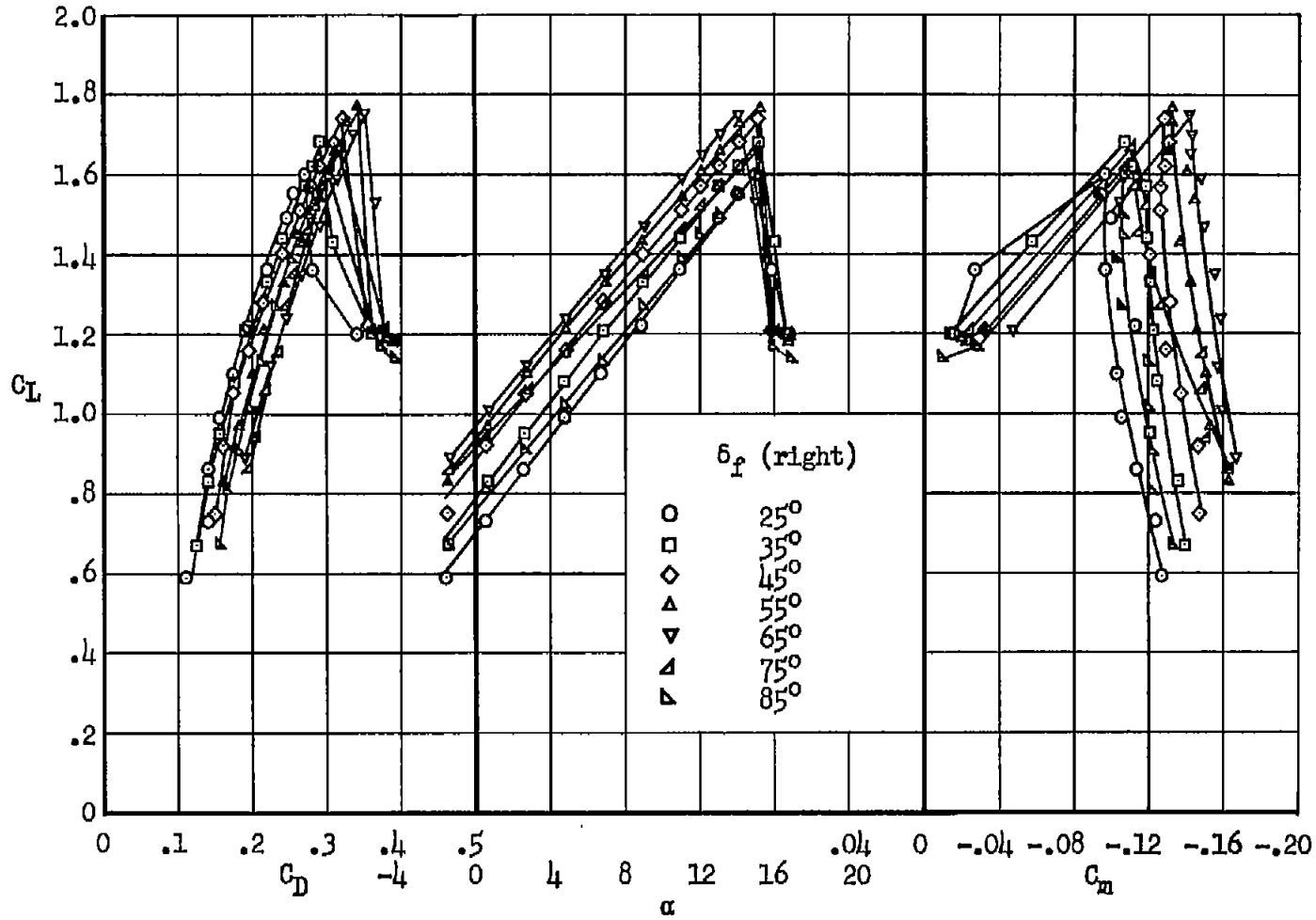

(a) Longitudinal characteristics.

Figure 24.- Effect of differential flap deflection on the aerodynamic characteristics of the airplane; δ_f (left) = 60°, $C_{\mu_R} = C_{\mu_L}$, $C_{\mu_R} + C_{\mu_L} = 0.017$, $\varphi = 30°$.

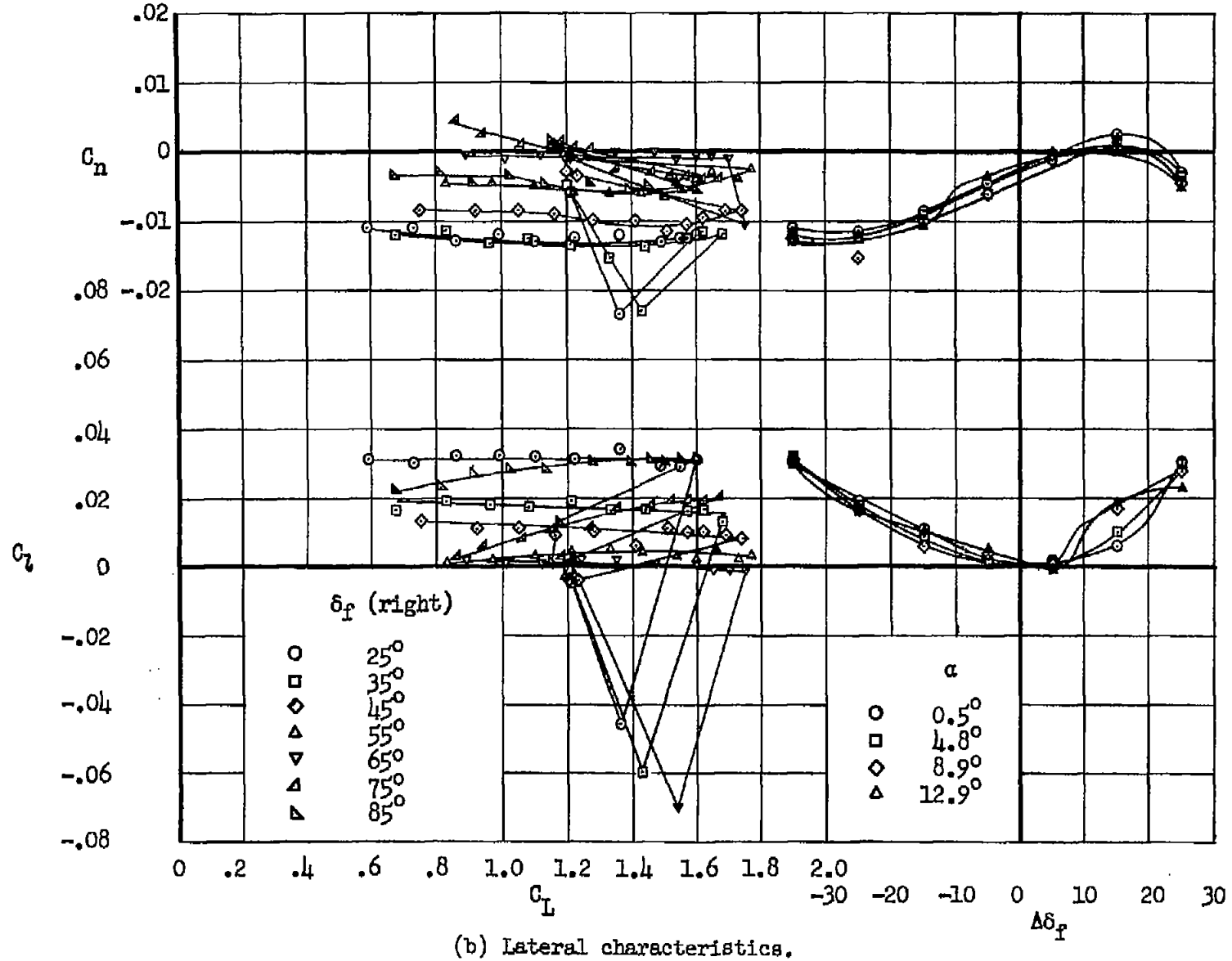

(b) Lateral characteristics.

Figure 24.- Concluded.

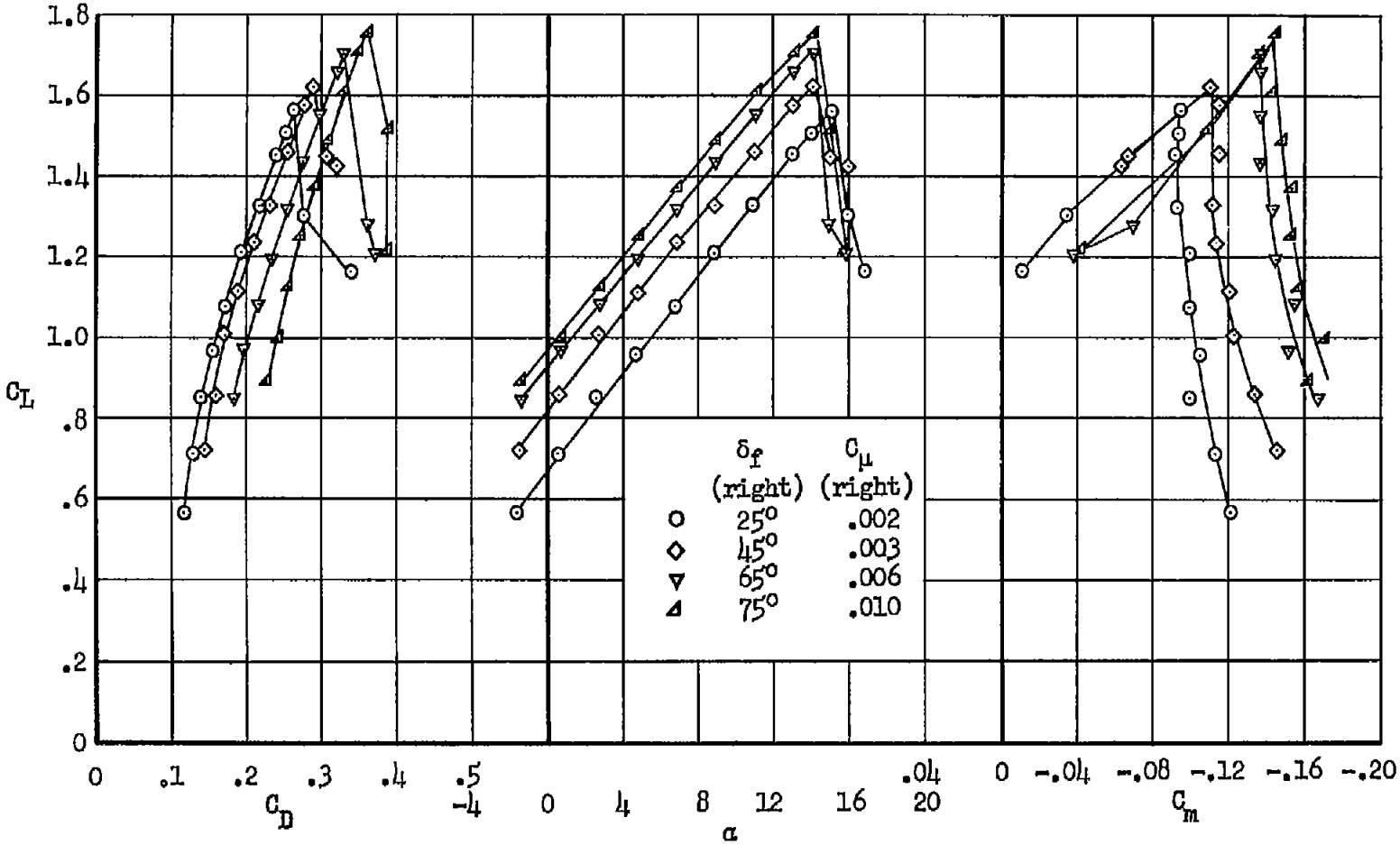

(a) Longitudinal characteristics.

Figure 25.- Effect of differentially deflected flaps with blowing increased with increasing flap deflection angle; δ_f (left) = 60°, C_μ (left flap) = 0.007.

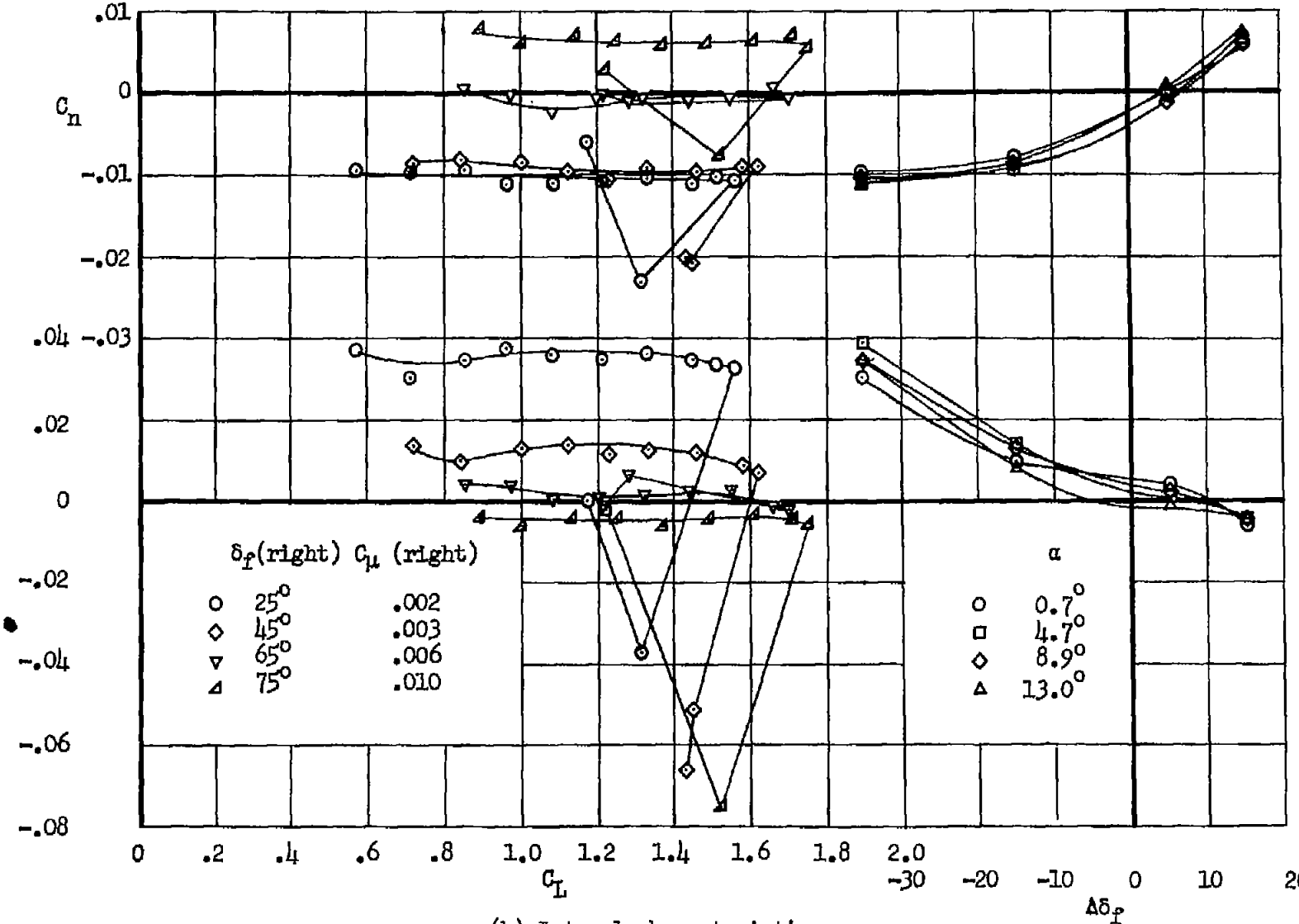

(b) Lateral characteristics.

Figure 25.- Concluded.

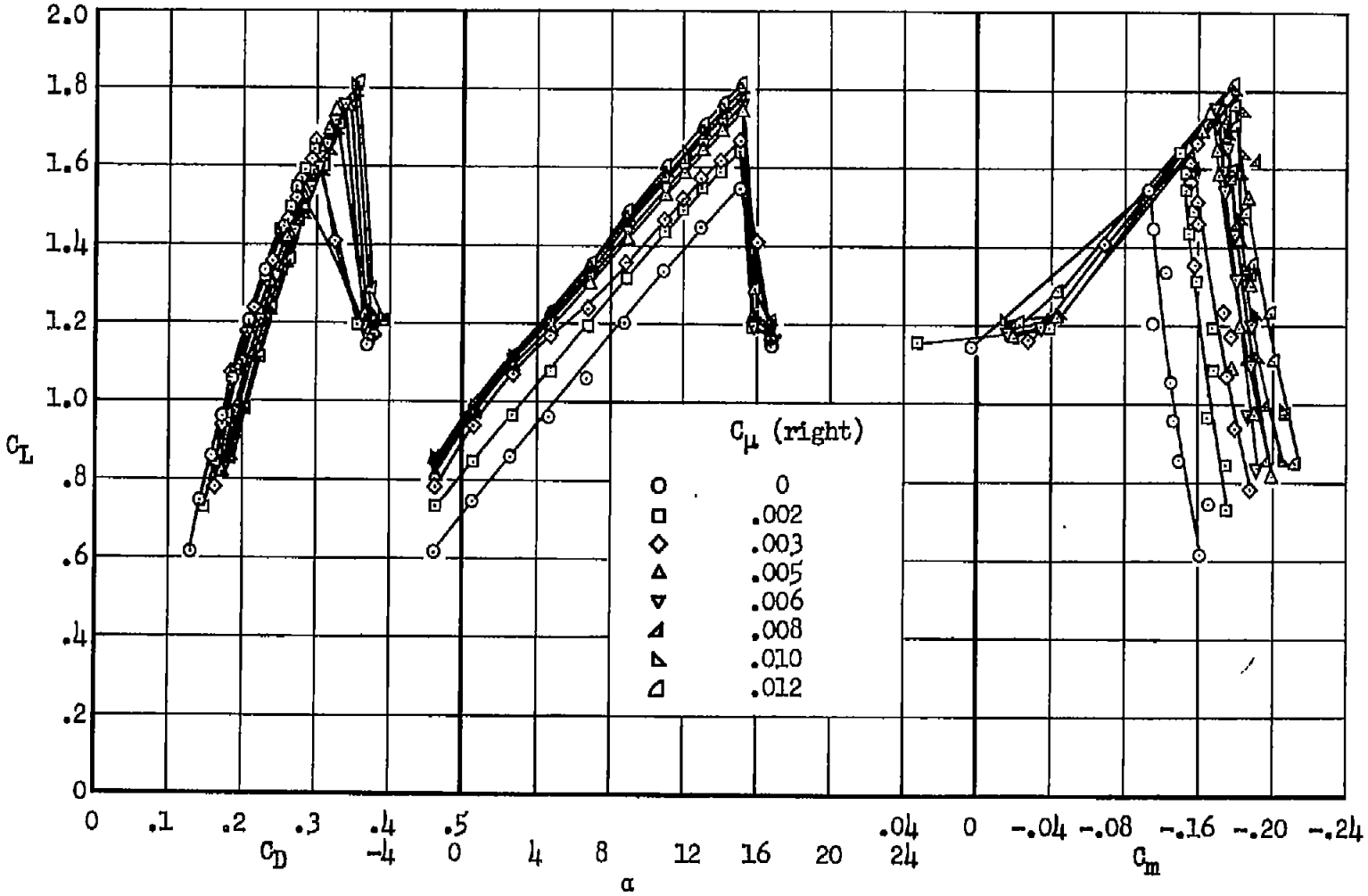

(a) Longitudinal characteristics.

Figure 26.- Effect of blowing differentially over the flaps; $\delta_f = 60^\circ$, C_μ (left) = 0.006.

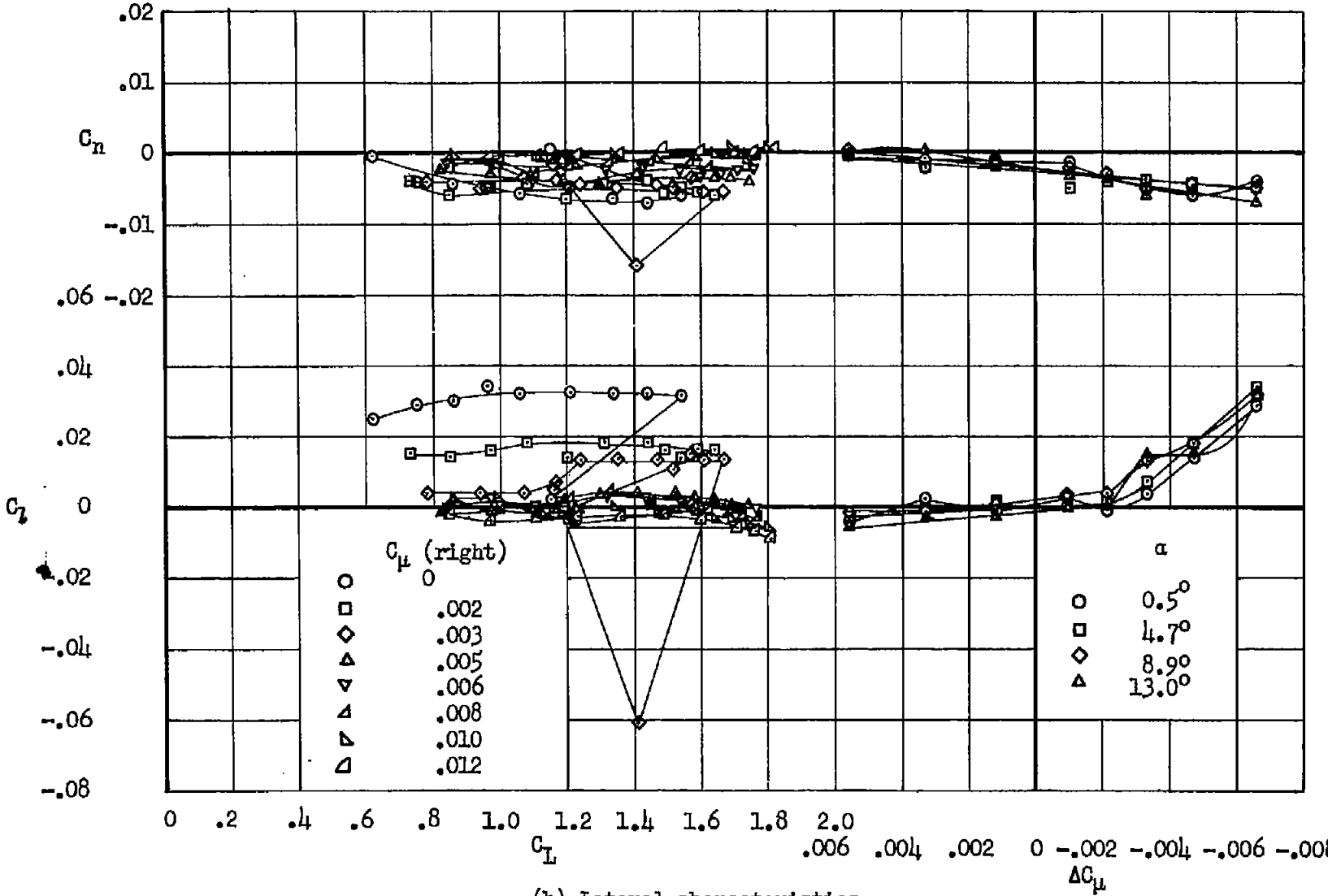

(b) Lateral characteristics.

Figure 26.- Concluded.

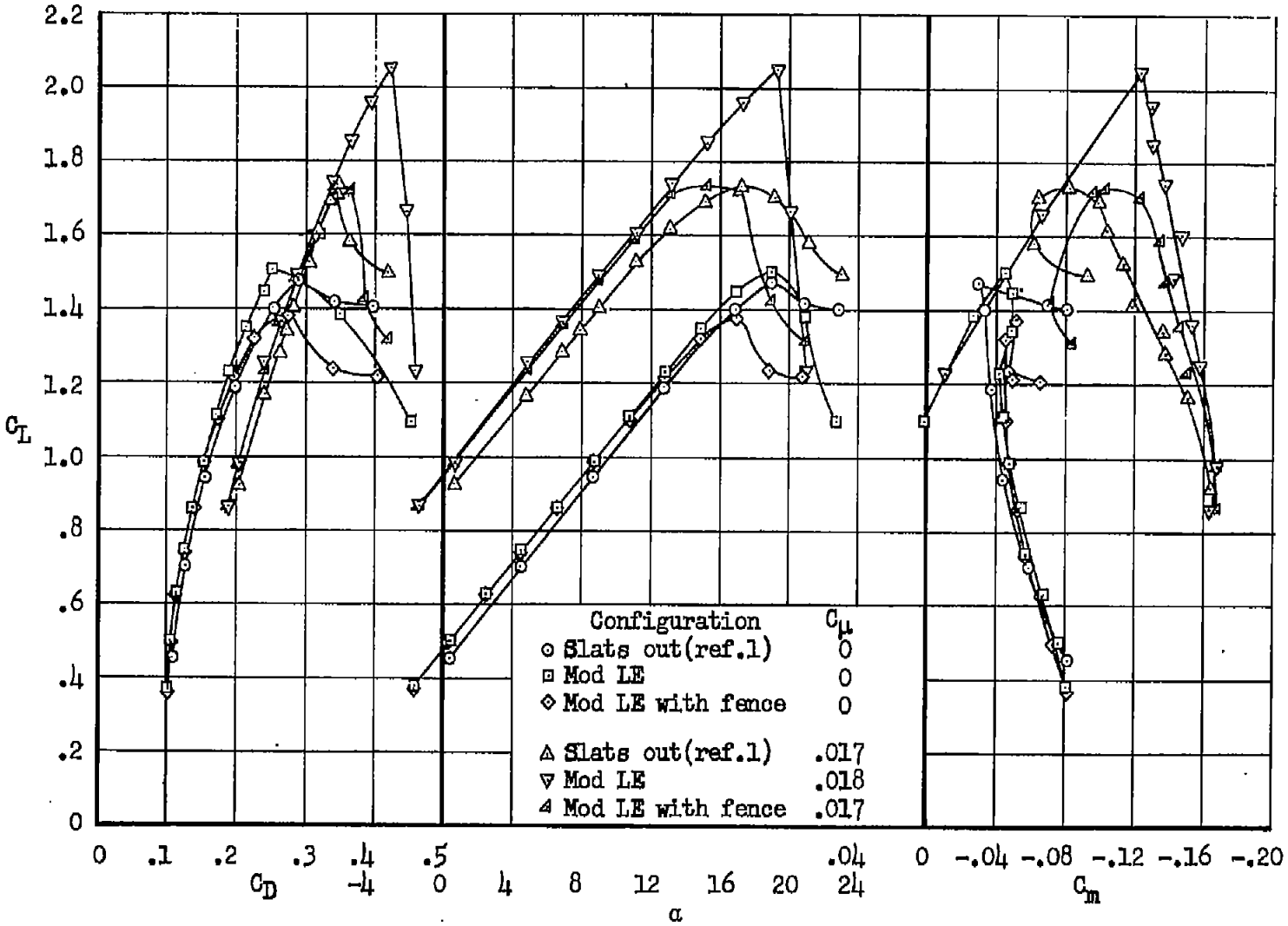

(a) Longitudinal characteristics.

Figure 27.- Aerodynamic characteristics of the airplane with the modified leading edge; $\delta_f = 60°$.

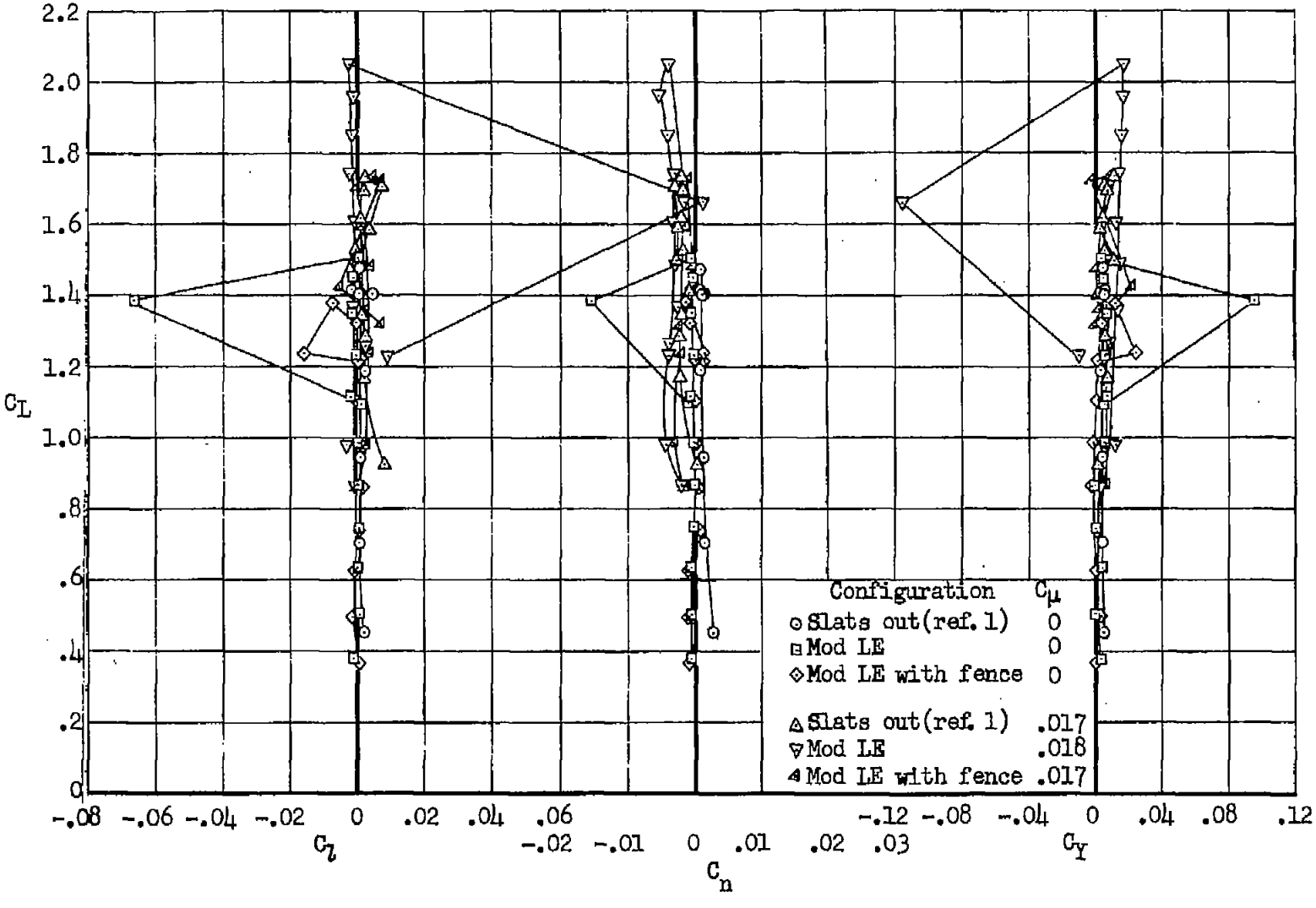

(b) Lateral characteristics.

Figure 27.- Concluded.